

Ceramic-based 3D printed bone graft in bone tissue reconstruction: a systematic review and proportional meta-analysis of clinical studies

Maria Apriliani Gani, Honey Dzikri Marhaeny, Gyubok Lee, Siti Farah Rahmawati, Putu Diah Apri Anjalikha, Timothy Sugito, Ronan Lebullenger, I Ketut Adnyana, Kangwon Lee & Damien Brézulier

To cite this article: Maria Apriliani Gani, Honey Dzikri Marhaeny, Gyubok Lee, Siti Farah Rahmawati, Putu Diah Apri Anjalikha, Timothy Sugito, Ronan Lebullenger, I Ketut Adnyana, Kangwon Lee & Damien Brézulier (18 Apr 2025): Ceramic-based 3D printed bone graft in bone tissue reconstruction: a systematic review and proportional meta-analysis of clinical studies, Expert Review of Medical Devices, DOI: [10.1080/17434440.2025.2492232](https://doi.org/10.1080/17434440.2025.2492232)

To link to this article: <https://doi.org/10.1080/17434440.2025.2492232>

 View supplementary material [↗](#)

 Published online: 18 Apr 2025.

 Submit your article to this journal [↗](#)

 Article views: 9

 View related articles [↗](#)

 View Crossmark data [↗](#)

META-ANALYSIS



Ceramic-based 3D printed bone graft in bone tissue reconstruction: a systematic review and proportional meta-analysis of clinical studies

Maria Apriliani Gani^{a,b}, Honey Dzikri Marhaeny^c, Gyubok Lee^d, Siti Farah Rahmawati^a, Putu Diah Apri Anjalikha^a, Timothy Sugito^a, Ronan Lebullenger^e, I Ketut Adnyana^a, Kangwon Lee^{d,f} and Damien Brézulier^{e,g}

^aDepartment of Pharmacology-Clinical Pharmacy, School of Pharmacy, Bandung Institute of Technology, Bandung, Indonesia; ^bBioscience and Biotechnology Research Center, Bandung Institute of Technology, Bandung, Indonesia; ^cDepartment of Pharmacy Practice, Faculty of Pharmacy, Airlangga University, Surabaya, Indonesia; ^dDepartment of Applied Bioengineering, Research Institute for Convergence Science, Seoul National University, Seoul, Republic of Korea; ^eInstitut des Sciences Chimiques de Rennes (ISCR) UMR 6226, Univ Rennes, Rennes, France; ^fResearch Institute for Convergence Science, Seoul National University, Suwon, Republic of Korea; ^gCHU Rennes, Pole Odontologie, Univ Rennes, Rennes, France

ABSTRACT

Introduction: This systematic review and proportional meta-analysis aims to evaluate the postoperative complication rate (CR%) of ceramic-based 3D-printed bone grafts based on the reported scientific articles conducted with human individuals.

Methods: MEDLINE and SCOPUS were used as information sources. The synthesis of the study was carried out from studies with human individuals and the use of 3D-printed bone graft-ceramic as inclusion criteria. Cohen's kappa (κ) was calculated for interrater reliability. Qualitative analysis was performed based on the characteristics and outcomes of the individual study, and quantitative analysis was performed using proportional meta-analysis for CR%.

Results: A total of 1352 records were identified through databases and resulted in 11 included studies ($\kappa = 0.81-1.00$) consisting of prospective clinical trials (64.63%), case series (16.67%), and case reports (18.18%). The overall postoperative complication rate was 14.3% (95% CI: 0.19-53.6). The postoperative complication rate for studies conducted on the cranial defect, the maxillofacial-zygomatic defect, and the tibial-femoral defect was 2.7%, 11.1%, and 15.6%, respectively. This review also highlights common 3D printing techniques, materials, and grafts' characteristics, as well as their clinical applications.

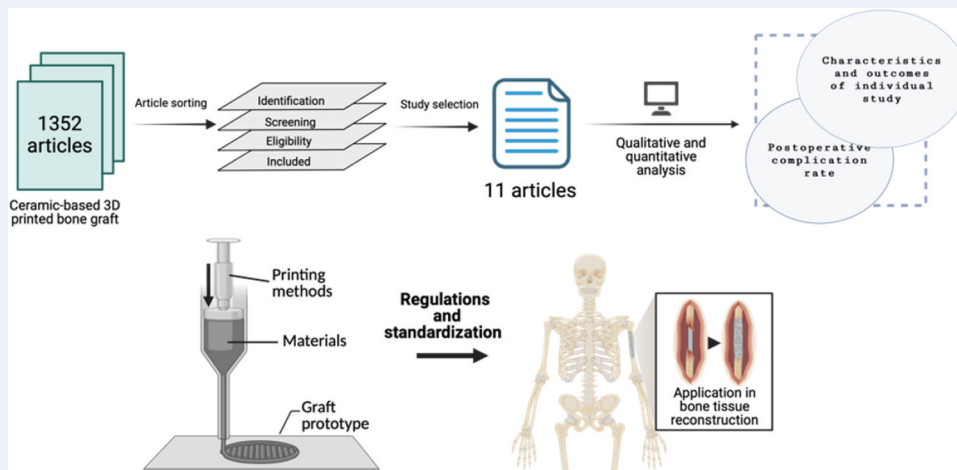
Conclusions: Ceramic-based 3D-printed bone grafts show potential as alternatives for bone tissue reconstruction.

ARTICLE HISTORY

Received 29 September 2024
Accepted 2 March 2025

KEYWORDS

Hydroxyapatite; tricalcium phosphate; ceramics; polylactic acid; polycaprolactone; bone scaffold; additive manufacturing; bone regeneration



1. Introduction

Bone defects are serious tissue injuries that result from pathological circumstances, such as trauma, infections, and tumors [1]. Bones can heal themselves through self-healing mechanisms

under suitable physiological and environmental conditions [1,2]. Secondary healing accounts for most fracture healing and is dependent on osteogenesis, osteoinduction, and osteoconduction factors. Osteoprogenitor cells that differentiate into osteoblasts

CONTACT Maria Apriliani Gani  maria.gani@itb.ac.id  Department of Pharmacology-Clinical Pharmacy, School of Pharmacy, Bandung Institute of Technology, Bandung 40132, Indonesia; Damien Brézulier  damien.brezulier@univ-rennes.fr  Institut des Sciences Chimiques de Rennes (ISCR) UMR 6226, Univ Rennes, Rennes 35700, France

 Supplemental data for this article can be accessed online at <https://doi.org/10.1080/17434440.2025.2492232>

and osteoclasts are specifically provided by mesenchymal stem cells, which are found in the bone marrow, granulation tissue, periosteum, surrounding soft tissues, and blood vessels. Osteoinductive factors (pro-inflammatory cytokines, growth factors, angiogenic factors, etc.) are transported to the fracture site by the vasculature and stimulate this differentiation, while osteoconduction is provided by the hematoma and cartilage callus [3]. Despite this robust function of osteoinductive factors, conditions such as large bone defects have a poor healing process due to the large size of the defect (2.5 cm or greater) and limited vascularization in the injured tissue. As a result, bones cannot heal spontaneously during a patient's lifetime [3,4]. Since there is quite a large loss of bone tissue, a support that is strong enough mechanically is needed to support the lost tissue with expectations that natural healing of the tissue can occur.

Limitations in the natural healing of bone defects in critical-sized cases necessitate specialized treatment in which the bone implant used must be anatomically compatible with the patients. 3D printing has grown exponentially in recent decades in healthcare. This additive manufacturing paradigm unleashes significant design freedom, making the technique perfectly suited for fabricating patient-specific anatomic models [5]. The application of 3D-printed devices, such as bone grafts, has been proven to improve functional and aesthetic outcomes while shortening surgery time [6,7]. This technique also does not cause donor site morbidity as commonly found in autologous techniques and is favored by both patients and surgeons [8,9]. It is predicted that by 2028, the patient-specific 3D-printed medical devices market will vastly grow and reach \$6.9 billion with an annual growth rate of 17.1% [10].

Ceramics are widely used as bone grafts due to their inertness and biocompatibility [11,12]. Ceramics, such as β -tricalcium phosphate (β -TCP) and hydroxyapatite (HA), have been shown to have positive impacts on bone regeneration whether used alone or as composites [13,14]. However, ceramics are recognized for their fragile characteristics [11,15]. As a result, using ceramic as a single material in bone reconstruction is ineffective, especially in load-bearing applications [11]. Combining biodegradable polymers offers an alternative to improved ceramic-based characteristics. Poly(lactic acid) (PLA) continues to be a favorable material for tissue engineering and bone fixation devices due to its biocompatibility, full biodegradability, and high stiffness [16]. A systematic review by Alonso-Fernández *et al.* [17] aimed to investigate the use of PLA/ceramics bone grafts in animal studies. The author detailed the biocompatibility and mechanical resistance of PLA/ceramics-based bone grafts have potential in clinical applications [17]. However, in recent years, the use of another biocompatible and biodegradable polymer called poly(ϵ -caprolactone) (PCL) is starting to dominate the bone regeneration field [16]. PLA and PCL differ in physical and mechanical properties, such as density, glass transition temperature, and melting temperatures [18,19]. This influences the end-point features of PLA/PCL-based bone grafts and how they perform in the *in vivo* environment which may influence the selection of the materials [17,20].

Unlike autologous bone grafts, 3D-printed bone grafts are still foreign to the host and may elicit an intense immune reaction. For example, HA is substantially more crystalline

than bone mineral, which makes HA-based implants substantially less resorbable and was reported to induce inflammatory responses [11,21,22]. Other than HA, PLA is also an FDA-approved material and is used as a thermoplastic polymer in the 3D printing technique. However, PLA breaks down into lactic acid which may induce excessive inflammatory responses [18]. Because of this, further investigation is needed to evaluate the safety of ceramic-based 3D-printed bone grafts from the existing studies in humans.

To the best of our knowledge, no reviews have reported postoperative complications in the use of ceramic-based 3D-printed bone grafts in humans. Here, we systematically review the use of ceramic-based 3D-printed bone grafts in humans and statistically analyze the proportion of postoperative complication rate by using proportional meta-analysis. We used proportional meta-analysis because this type of analysis focuses on estimating the overall proportion, for example, the survival rate [23] or nonunion rate in the use of particular grafts [24]. We are also delving deeply into the commonly used 3D printing methods, the character of the most used materials, and how they influence the choice of materials for clinical applications. This review will pave the path for the commercialization and clinical applications of ceramic-based 3D-printed bone grafts, as well as for the potential replacement of autologous bone grafts as the 'gold standard' in clinical practices with 3D-printed bone grafts.

2. Methods

2.1. Protocol and registration

This review is to evaluate the postoperative complication rate (CR%) of ceramic-based 3D-printed bone grafts based on the reported scientific articles conducted with human individuals. We perform a systematic review before meta-analysis to comprehensively identify the evidence. The systematic review was conducted and reported following the Preferred Reporting Items for Systematic Reviews and Meta-Analyses (PRISMA) guidelines [25,26]. The review protocol was registered on the International Prospective Register of Systematic Reviews (PROSPERO) database with ID CRD42023478050. This study did not require ethical approval or informed consent.

2.2. Eligibility criteria

Eligibility criteria were considered concerning all human studies with population, intervention, comparator, and outcome (PICO) framework as presented in Table 1. The focused question of this review was 'Is ceramic-based 3D printed bone graft safe in clinical application?'

2.3. Information sources

The electronic databases used were MEDLINE (PubMed) and SCOPUS. Hand searches were also performed on the authors' electronic library and the references in the included articles. The final update for all electronic searches was completed on 18 October 2023.

Table 1. Search strategy and criteria for inclusion.

Search terms	Population	#1 – ((clinical study) OR (clinical trial) OR (RCT) OR (human) OR (subject) OR (participant))
	Intervention	#2 – ((3D print*) OR (3D bone) OR (fused deposition modelling) OR (selective laser sintering) OR (stereolithography) OR (digital light processing) OR (3D gel printing)) AND ((ceramic OR (hydroxyapatite) OR (alumina) or (tricalcium phosphate) OR (zirconium oxide) OR (barium titanate) OR (silicon carbide) OR (silica carbide) OR (ferrite) OR (calcium silicate) OR (calcium carbonate))
	Comparison	#3 – ((transplantation) OR (autologous) OR (autografts) OR (tissue scaffold) OR (tissue harvesting) OR (organ harvesting))
	Outcome	#4 – ((bone regeneration) OR (bone formation) OR (graft rejection) OR (bone gain) OR (intraoperative complications) OR (postoperative complications) OR (complication) OR (side effect) OR (adverse effect) OR (treatment failure) OR (graft failure))
Search combination		#1 AND #2 AND #3 AND #4
Publication year		1 January 2000 to 26 September 2023
Database search	Electronic Journals	PubMed, SCOPUS
Selection criteria	Inclusion criteria	All peer-reviewed journals available in PubMed and SCOPUS. No filters were applied for the journals.
	Exclusion criteria	The study must be human studies (such as prospective clinical trials, case series, and case reports). The intervention must be a 3D-printed bone graft with ceramic as the main or substitute material that is used at any location related to the bone defect. The study must report if the intervention causes postoperative side effects or not.
		<i>In vitro</i> , <i>in vivo</i> , <i>in silico</i> studies, literature review, and study protocol.

2.4. Search strategy

The initial search technique was designed and implemented by MAG and HDM. The search terms used are presented in Table 1. The search terms were combined with 'AND' and limited to articles published between 1 January 2000, and 26 September 2023. The search was then discussed by MAG, HDM, and IKA to confirm the number of discovered articles.

2.5. Study selection

Studies that met the inclusion criteria were included in this review (Figure 1, Table 2). Initial title and abstract screening were performed independently by MAG and HDM. The final list of studies for full-text analysis and data extraction was provided only after

the two investigators reached an agreement. Disagreements were resolved via a consensus discussion with IKA. Cohen's kappa (κ) was calculated for interrater reliability between investigators by using SPSS version 24.0 software (IBM Corporation, U.S.A.). During the study selection, studies that used other methods to fabricate personalized bone grafts were also included in separate tables in the data collection process to provide a border overview.

2.6. Data collection

MAG and HDM independently extracted the data from the included studies based on the required parameters and information that have been previously agreed between MAG, HDM, and IKA. This was related to the descriptive patient/population level information (e.g. sample size, mean patient age, gender

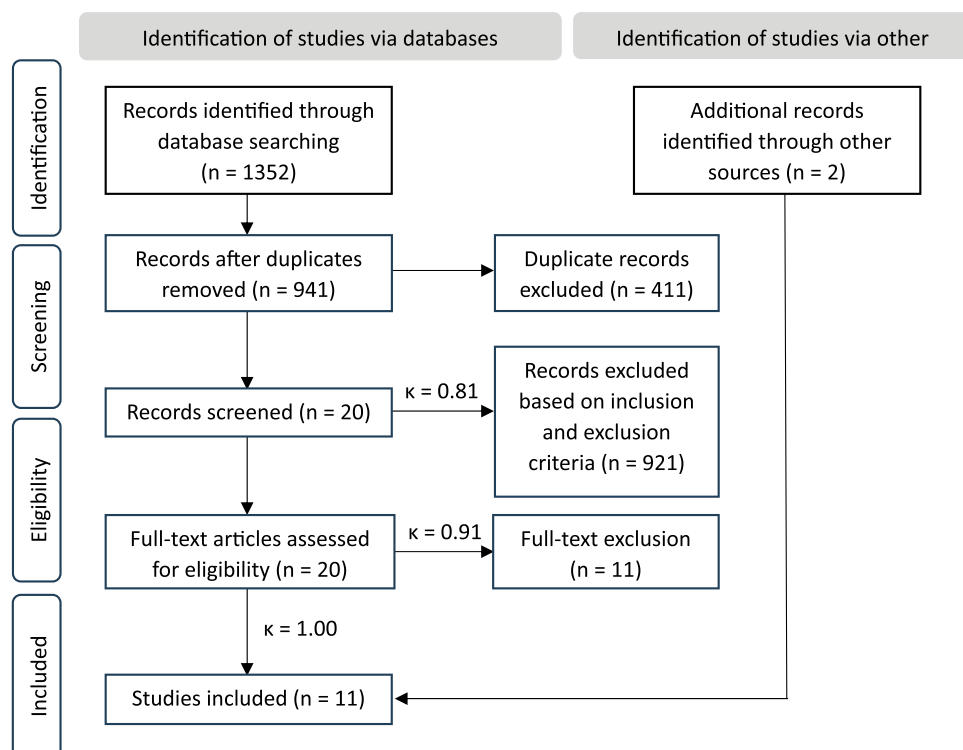
**Figure 1.** The flow-chart of study inclusion.

Table 2. The main reason for exclusion after full-text screening.

Main reason	Number (n)	References
Did not use 3D printing technology	9	[27–34]
Not human study	1	[35]
Did not report postoperative complications	1	[36]

distribution), treatment and fabrication technique, and study outcomes. Disagreements were resolved through discussion.

2.7. Missing data

Missing information regarding postoperative complications was requested through e-mail to the corresponding author of the study. In case of a non-response, the study was excluded.

2.8. Statistical analysis

A fixed effect was performed to determine the proportion of postoperative complication rate (CR%). Each study's data was extracted with 95% confidence intervals (95% CI) and analyzed using JAMOV software version 2.3.28.0 (retrieved from <https://www.jamovi.org>). We also analyzed CR% of studies that examined 3D graft implantation for 1) cranial bone, 2) maxillofacial-zygomatic bone, and 3) tibial-femoral bone with 95% CI performed on the same software. I^2 statistics were used to assess heterogeneity, with the following interpretation guide: 0% to 25% indicate low heterogeneity; 25% to 75% indicate moderate heterogeneity; and 75% to 100% indicate significant heterogeneity. Funnel plots were created to test for publication bias.

2.9. Risk of bias of the included articles

The quality of each study was assessed independently by MAG and HDM. The study design of each included study was different. Thus, the quality assessment was conducted by using assessment instruments that matched the study design. Prospective studies with no control group were assessed by using NIH's Study Quality Assessment Tools for Before-After (Pre-Post) Studies With No Control Group, case series studies were assessed by using NIH's Study Quality Assessment for Case Series Studies, while case report studies were assessed by using critical assessment instruments from the Joanna Briggs Institute (JBI) for case reports. In case of disagreement, a third reviewer's opinion (IKA) was sought for further discussion to reach an agreement [37,38].

3. Results

3.1. Study selection

The selection process of this systematic review was based on the PRISMA guidelines (Figure 1). Initial search from databases delivered 752 and 600 studies from SCOPUS and PubMed, respectively, which made 1352 records in total. Title and abstract screened excluded 921 studies and 20 remaining studies were assessed for full-text screening. The reason for full-text exclusion is present in Table 2: Nine studies did not use 3D printing technology to fabricate the intervention used

and/or did not conduct 3D printing on the ceramic material but on other supporting devices used in the treatment, such as titanium mesh or reconstruction plates for bone [27–34,39]. One study is not a human study [35] and one study did not report postoperative complications after bone graft operation surgery. On the other hand, manual searches were also performed on the authors' library and references in the included articles, this resulted in two articles that were also included in the review [7,40]. Studies that used other methods to fabricate 3D bone grafts were also listed in Supplementary 3 and 4 to provide a border overview of personalized bone grafts.

3.2. Study characteristics

Of the 11 included studies, 7 studies (64.63%) are prospective clinical trials, 2 studies (16.67%) are case series, and 2 studies (18.18%) are case reports (Table 3). For studies that used other manufacturing methods, 5 studies (71.43%) are prospective clinical trials and 2 studies (28.57%) are case reports (Supplementary 3).

3.3. Qualitative analysis of the included studies

TCP was the most used ceramic in 3D-printed bone grafts in the included studies (81.81%), with 3 studies using α -TCP (27.27%), 2 studies using β -TCP (18.18%), and 4 other studies used TCP but did not report the form of TCP (36.36%). HA and BGS-7 were also used in one study, respectively (each counts 9.09%). Combination material was also used in the included studies with PCL count as the most used material (6 studies, 54.54%), and resin in one study in combination with HA (9.09%, Table 3). Moreover, 85.71% of studies that used other methods used HA ceramic, while one study used BCP (14.29%). The method used in these studies was CNC in 4 studies (57.14%), molding in 2 studies (28.57%), and cutting in one study (14.29%, Supplementary 3).

All eleven studies reported information regarding postoperative complications after bone graft treatment. Infection was the most common postoperative event with five cases. Events such as redness swelling and scaffolding failure also occurred (Table 4). For studies that used other methods to fabricate 3D bone grafts, postoperative complications vary, such as dehiscence of the bone grafts, scalp thinning, pain, hyperesthesia, and others (Supplementary 4). Outcomes related to bone regeneration vary between studies as presented in Tables 4 and Supplementary 4.

3.4. Proportional meta-analysis of the included studies

No study included a negative or positive control group. Thus, we presented the statistical analysis as a proportional meta-analysis. The overall postoperative complication rate was 14.3% (95% CI: 0.19–53.6, Figure 2). A low level of heterogeneity was found among the studies ($I^2 = 0\%$, $p = 0.763$ $n = 11$; Figure 2). A funnel plot analysis was performed to investigate potential publication bias (Supplementary 1). Furthermore, the postoperative complication rate for studies conducted on cranial defect was 2.7% (95% CI: 8.7–14.0, Figure 3), the maxillofacial-zygomatic defect was 11.1% (95% CI: 1.54–20.6,

Table 3. Characteristics of the included studies.

Study	Country	Study design	Type of defect	Treatment type	Software	Device	Sample size (n)		Mean age (years)	Gender (n)	
							Patient	Region		Female	Male
Saijo 2009	Japan	Prospective clinical trial	Maxillofacial	α -TCP	NS	Z406 3D (Z-Corporation, U.S.A.)	10	10	35.0 (18–55)	9	1
Probst 2010	Germany	Case report	Cranial	PCL/TCP	Mimics (Materialise, Belgium)	FDM3000® (Stratasys Inc., U.S.A.)	1	1	11.0	NS	NS
Brie 2013	France	Prospective clinical trial	Cranial	Resin/HA	NS	NS	8	8	44.1 (27–63)	2	6
Kanno 2016	Japan	Prospective clinical trial	Maxillofacial	α -TCP-sodium chondroitin sulfate-disodium succinate (termed as CT-bone)	Mimics (Materialise, Belgium)	Z406 3D (Z-Corporation, U.S.A.)	20	20	31.7 (18–55)	14	6
Saijo 2016	Japan	Prospective clinical trial	Maxillofacial	α -TCP	NS	Z406 3D (Z-Corporation, U.S.A.)	20	23	31.7 (18–55)	14	6
Kobbe 2020	Germany	Case report	Femoral	PCL/TCP combined with autologous bone graft and BMP-2	NS (procced by Osteopore®)	NS (procced by Osteopore®, Singapore)	1	1	29.0	NS	NS
Lee 2020	South Korea	Prospective clinical trial	Zygomatic	CaOSiO ₂ -P2O ₅ -B2O ₃ glass-ceramic (BGS-7)	3 Matics (Materialise, Belgium)	NS (procced by Osteopore®)	10	10	36.0 (24–53)	9	1
Castrisos 2022	Australia	Case series	Maxillofacial	PCL/TCP	3 Matics (Materialise, Belgium)	NS (procced by Osteopore®)	1	1	12	1	-
			Tibial	PCL/TCP	3 Matics (Materialise, Belgium)	NS (procced by Osteopore®)	2	2	21.5 (16–27)	1	1
			Cranial	PCL/TCP	3 Matics (Materialise, Belgium)	NS (procced by Osteopore®)	1	1	25	-	1
Jeong 2022	South Korea	Prospective clinical trial	Zygomatic, maxillary	PCL/ β -TCP	3 Matics (Materialise, Belgium)	NS	8	8	36.4 (19–51)	4	4
Laubach 2022	Germany-Australia	Case series	Femoral, tibial	PCL/TCP combined with autologous bone graft	Geomagic (3D Systems, U.S.A.) or Autodesk Meshmixer (Autodesk Inc., U.S.A.)	NS (procced by Osteopore®)	4	4	30.5 (23–42)	NS	NS
Park 2022	South Korea	Prospective clinical trial	Cranial	PCL/ β -TCP	Mimics (Materialise, Belgium)	NS (procced by TnR T&R Biofab, South Korea)	7	7	34.3 (20–62)	NS	NS

α -TCP, alpha-tricalcium phosphate; β -TCP, beta-tricalcium phosphate; PCL, polycaprolactone; NS, not specified.

Figure 4), the tibial-femoral defect was 15.6% (95% CI: 16.2–47.4, Figure 5).

3.5. Risk of bias of the included articles

The results of the quality assessment of the included studies are shown in Supplementary 2. The included studies are considered to have good/fair quality with a low risk of bias.

4. Discussion

This review demonstrates that a variety of techniques are employed to create 3D ceramic-based bone grafts in the clinical trials that have been documented thus far. This proportional meta-analysis found that the total postoperative complication rate for 3D ceramic-based bone grafts was 14.3%, while the postoperative complication rate for studies conducted on the cranial defect, the maxillofacial-zygomatic defect, and the tibial-femoral defect was 2.7%, 11.1%, and 15.6%, respectively. The benefit of utilizing a 3D-printed bone graft is that there is no

donor site morbidity, which is known to play a significant part in postoperative problems with autologous bone grafts [8,9]. Here, we discussed in detail the fabrication methods that have been used to produce 3D ceramic-based bone grafts, their characteristics, as well as their performance in bone healing.

4.1. Fabrication technique for custom-made 3D bone graft

The fabrication technique used to produce 3D bone grafts varies between clinical investigations included in this review. In this section, here we discussed in detail the general fabrication method of 3D bone grafts, which includes conventional cutting or molding methods, layer-by-layer 3D printing without biological material, and layer-by-layer 3D printing with biological materials.

4.1.1. Cutting or molding methods

Non-layer-by-layer fabrication is one technique to produce customized 3D bone grafts. By using the computer numerical

Table 4. Outcomes of individual study.

Study	Months of follow-up, mean (range)	Assessment method	Parameter	Outcomes	
				Parameter	Results
Saijo 2009	6, 12	CT scan, clinical symptom	Intraoperative complications Postoperative complications Compatibility Bone union after 12 months Satisfaction	NM 0/10 patients 10/10 patients 10/10 patients 10/10 patients	
Probst 2010	6, 9, 12	CT scan, clinical symptom	Intraoperative complications Postoperative complications Overall result	NM Not present The scaffold was well integrated and beginning bony consolidation was detected.	
Brie 2013	1, 6, 12	CT scan, clinical symptom	Intraoperative complications Postoperative complications Satisfaction	NM 0/8 patients (in terms of infection or fracture of the implant) 8/8 patients	
Kanno 2016	36.555 (12–87)	CT scan, clinical symptom	Intraoperative complications Postoperative complications after 1 year Postoperative complications after 1–5 years Compatibility Chronological change Bone union Satisfaction	NM 0/20 patients 4/20 patients Infections were present in 4 sites of 4 patients which made the CT bone removed 23/23 sites 0/23 sites 18/21 sites 18/20 patients	
Saijo 2016	55.526 (13–115)	CT scan, clinical symptom	Intraoperative complications Postoperative complications	NM 5/20 patients An artificial bone of 1 patient was broken, 1 patient was an MRSA carrier and infection occurred early after surgery, patients experienced redness and swelling on the implantation regions	
Kobbe 2020	12	CT scan, X-ray, clinical symptom	Intraoperative complications Postoperative complications Bony fusion	NM Not present Almost complete	
Lee 2020	6	CT scan, clinical symptom	Intraoperative complications Postoperative complications Bone fusion Immobilization Satisfaction	NM 0/10 patients 10/10 patients, average fusion rate of 76.97% (58.33–88.24%) Average displacement 0.415 mm (0.1155–0.889 mm) 9/9 patients, 1 patient lost to follow-up	
Castrisio 2022	15.3 (4–35)	CT scan, X-ray, clinical symptom	Intraoperative complications Postoperative complications	0/4 patients 1/4 patients 1 patient had extensive blistering of the native skin distal to the CPCF skin paddle on postoperative day two (tibial defect)	
Jeong 2022	6	CT scan, clinical symptom	Intraoperative complications Postoperative complications Volume conformity Bone volume fraction Tissue density	NM 1/8 patients 1 patient had wound dehiscence due to delayed wound healing Mean of 79.71% (70.89–86.31) Mean of 23.34% (7.81–66.21) Mean of 188.84 hU (151.48–291.74)	
Laubach 2022	15.250 (8–23)	CT scan, X-ray, clinical symptom	Intraoperative complications Postoperative complications Compatibility Bony ingrowth Comprehensive bone regeneration and full weight-bearing	0/4 patients 0/4 patients 4/4 patients 3/4 patients 1/4 patients Present in the case with a 10 cm tibia shaft	
Park 2022	8.386 (6–17)	CT scan, clinical symptom	Intraoperative complications Postoperative complications Increased soft tissue volume at 2 weeks Increased soft tissue volume at 6 months Symmetry after surgery Smoothness on the implant edges	NM 1/7 patients 1 patient had a seroma at 3 months after operation 15.800 cm ³ (6.3–53.3) 14.871 cm ³ (6.3–48.7) 6/7 patients 1 patient had partial symmetry 6/7 patients 1 patient had a slightly irregular edge	

NM, not mentioned.

control (CNC) method, it is possible to automate the control of machine tools using software embedded in a computer to cut or mold a particular material [41]. In the screening and full-text assessment of our systematic review, we found 7 studies that

used the non-layer-by-layer fabrication method. References number [28,41–43] used the CNC milling technique, references number [44,45] used the molding technique, and references number [46] used the cutting technique (Supplementary 3).

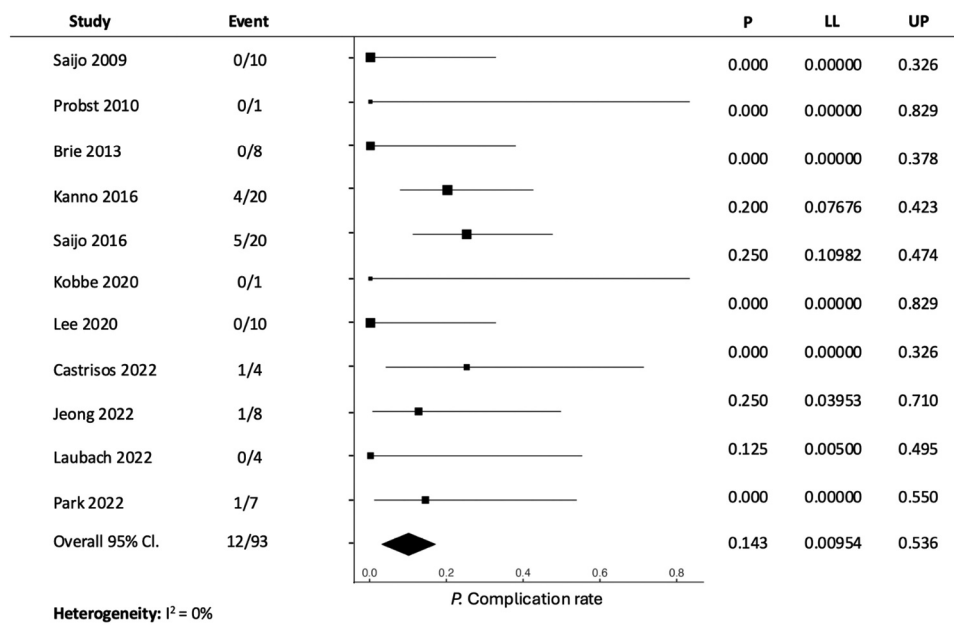


Figure 2. Forest plot showing postoperative complication rate % for all included studies (CI, confidence interval).

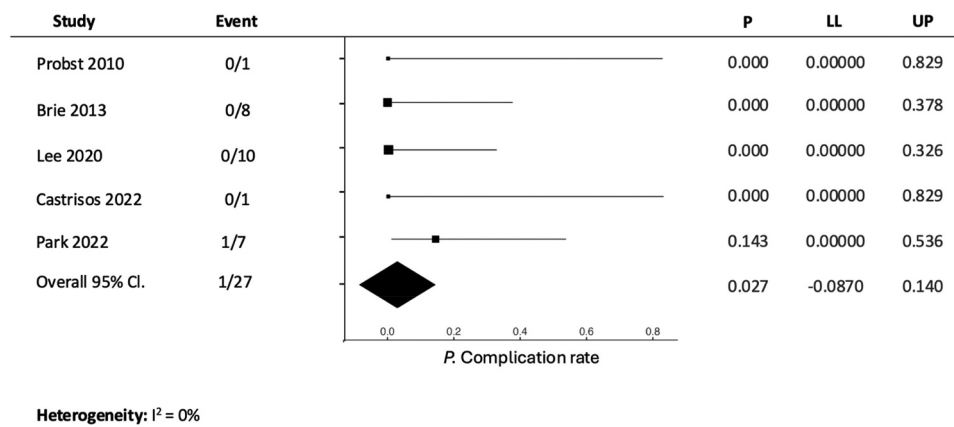


Figure 3. Forest plot showing postoperative complication rate % for cranial defect (CI, confidence interval).

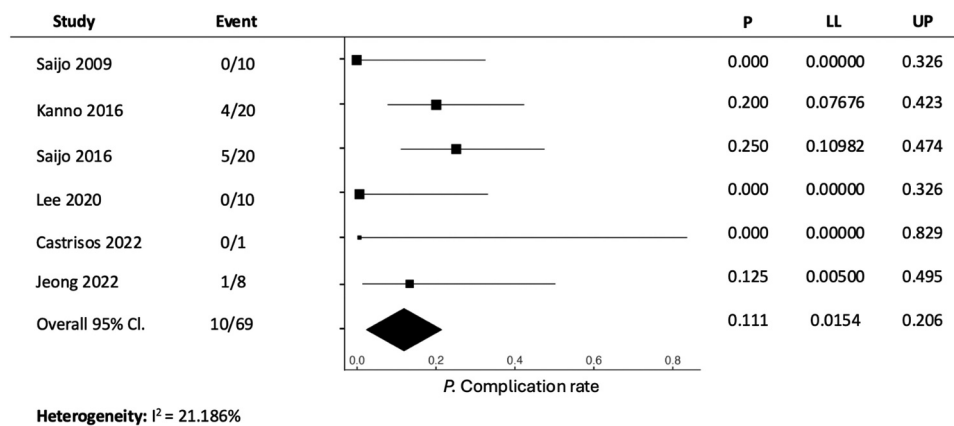


Figure 4. Forest plot showing postoperative complication rate % for maxillofacial-zygomatic defect (CI, confidence interval).

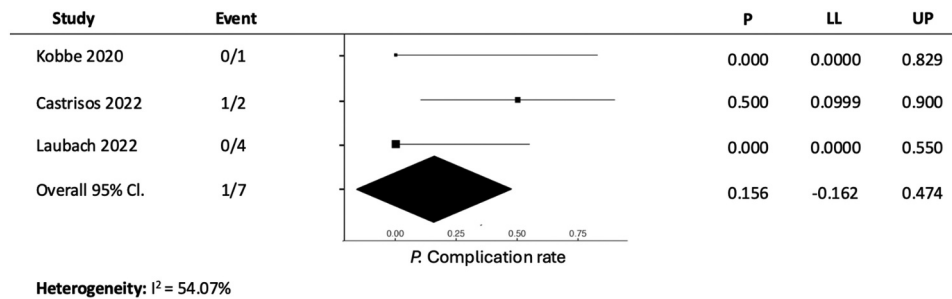


Figure 5. Forest plot showing postoperative complication rate % for tibial-femoral defect (CI, confidence interval).

The outcomes of each study are presented in Supplementary 4.

CNC milling technique uses porous ceramic blocks, such as HA [28,41] or BCP [42] to fabricate 3D bone grafts. This technique is great for shaping materials by generating small chip fragments [47]. However, since no layer-by-layer processing is applied, the porosity of the material is difficult to customize during the fabrication process. For instance [48], used gel casting foam to produce customized bone grafts by using a porous hydroxyapatite foam. The porosity of the graft was 83.3% and had an average compressive strength of 2 MPa. Fabris *et al.* [49] also fabricated zirconia grafts with periodic open cellular structures using CNC machining from zirconia blocks. Different drill sizes used in the study (1 to 2 mm diameter driller) produced bone grafts in distributed pore sizes with porosity starting from 39 to 57% with compressive strength starting from 667 MPa to 300 MPa, respectively [49]. This proved that controlled pore size and/or porosity of bone grafts fabricated by using this CNC machining can only be reached by using suitable drill sizes. Other than driller sizes, machining parameters such as spindle speed, feed rate, depth of cut, and machining direction were reported to have impacts on cutting force and surface roughness or ceramic matrix [50].

The bone graft performance made from the cutting/molding techniques varies between studies (Supplementary 3). The study by Mangano *et al.* [41] resulted in 1/10 postoperative complications. The authors reported that a patient experienced dehiscence of the graft two months after the reconstructive surgery [41]. Hardy *et al.* [46] also reported postoperative complications after HA graft implantation. However, there was no additional investigation if the complications were related to the bone graft or not. Only a study by Staffa *et al.* [45] reported that *Neisseria meningitidis* infection experienced by a patient was accelerated because of the grafts' porosity. This showed that bone graft characteristics closely determine the graft's performance in bone healing.

4.1.2. Layer-by-layer conventional 3D printing methods

During the past decades, there has been a shift in the use of conventional methods to layer-by-layer 3D printing methods in fabricating 3D ceramic-based bone grafts. For example, clinical investigation series from Mangano *et al.* [28,41,42] used the CNC milling technique to fabricate ceramic-based 3D bone grafts, however, years later, the researchers started using layer-by-layer 3D printing method to produce 3D BCP

bone grafts [36]. There have been several developed methods for layer-by-layer 3D printing. Here, we discussed in detail each method that has been used for bone tissue reconstruction.

4.1.2.1. Stereolithography (SLA) digital light processing (DLP).

SLA uses photosensitive resin material to fabricate 3D objects by controlling the laser through a computer. Surface scanning of the liquid photo resin occurs based on the specific information of the layer. The thin resin layer in the scanned area is cured by photopolymerization to form a thin layer of the part. After one layer is completed, the platform will move down and a new layer will be produced until the 3D part is obtained [51]. One advantage of SLA is its faster printing rate and excellent resolution [52]. The improvement of the SLA method is called digital light processing (DLP), which uses a single projector light source. A beam of light is used to pass across the layer of resin mixture all at once, which simplifies the printing process [52]. However, material choices are limited and expensive for this method [52].

Studies included in this review did not specify which kind of method was used to fabricate layer-by-layer 3D-printed bone grafts. However, other studies have proved that SLA can produce grafts with controlled porosity and pore sizes that result in desired mechanical strength. Sodeyama *et al.* [53] reported that a 3D polymer-infiltrated ceramic network made from SLA exhibited a nano-sized dual-network structure with a similar Vickers hardness to enamel, and a similar elastic modulus to dentin [53]. In fabricating bone grafts, SLA can also be combined with other methods. For example, Hann *et al.* [54] fabricated a biomimetic nano-bone tissue construct with a perfusable by combining SLA and FDM methods. Experiments in physiological conditions revealed that during up to 20 days of observation, the graft improved vascular network formation and osteogenic maturation of the structures [54]. This proved that SLA can produce grafts with specific characteristics that contribute to their beneficial action in physiological conditions.

4.1.2.2. Selective laser sintering (SLS) and selective laser melting (SLM).

SLS is a technology that heats powdery material such as wax or plastic powder to fabricate 3D objects. In this method, the powder is heated below its melting point and then flattened using a leveling stick [51]. Under computer control, the laser beam is selectively

sintered based on the delamination-specific information. After one layer is finished, the next layer is sintered, and any remaining powder is removed [51]. To obtain optimal sintering conditions for powders, parameters including laser power and scan speed should be optimized [55]. SLS can print a wide variety of materials and has fast processing speed as well as a high precision of the 3D graft. The advantage of SLS is also supports structures that can be easily removed [52]. Selective laser melting (SLM) is similar to SLS and was developed as an improvement. The primary distinction between them is the heating temperature range. SLS heats the powder surface slightly below the melting temperatures, while SLM heats the powder bed to the material's melting point [52].

SLS/SLM is widely used to print metals for reconstruction plates [56–58]. However, studies also started reporting the use of this method in printing 3D ceramic bone grafts. In combination with polymer, ceramic-based material can be printed with SLS/SLM. A study by Park *et al.* [59] compared SLS and extrusion-based methods in fabricating a 3D bone graft made from PCL and HA. The authors reported that printing modality had inherent characteristics that impact printing outcomes and eventually implant performance [59]. Another study also showed that HA and PCL printed by SLS showed favorable activities for bone cells [55]. However, SLS/SLM may destroy biological material and thus can not support tissue engineering applications [51].

4.1.2.3. Fused deposition modeling (FDM). Fused Deposition Modeling, also known as Fused Lamination Modeling, is a part of the extrusion method that employs a heater plug to melt and extrude filaments through the nozzle [51,52]. Similar to another 3D printing method, FDM uses computer controls to selectively coat the material on the workbench based on cross-sectional profile information [51]. After quick cooling, a cross-sectional layer develops. When one layer is completed, the machine table falls a height that is the thickness of the layer and then creates the next layer until the full solid frame is produced [51]. Because of this, the main material that should be used for this method is heat-shrinkable polymers, such as polylactic acid and polycaprolactone [11,21]. FDM is a simple and low-cost method for the fabrication of 3D bone scaffolds. However, it is not ideal for the accuracy of the printed prototype. The involvement of high temperatures in this method can destroy heat-sensitive material, making it non-applicable for the printing of growth factors, proteins, and cells that are mostly involved in tissue engineering [51].

Despite the fact that it can only print a limited number of materials, since it has low cost of manufacturing, FDM has been utilized to create a wide variety of 3D ceramic grafts, such as for HA [60], BCP [61], and TCP [62,63]. This method helps incorporate ceramics into existing bone grafts with various incorporation methods, for example by making filaments/blends containing various materials including ceramic, and using the filaments/blends for 3D printing, which was used by Kim *et al.* [64] with PCL and HA. On the other hand, other researchers used thermoplastic materials as a 'frame' before incorporating the ceramic into the 3D-printed frame with chemical reactions such as hydrolysis [65,66].

The success of this method in fabricating 3D-printed grafts has been widely reported. Wang *et al.* reported that FDM can produce PLA/nano β -TCP graft with desired internal pores and external structures [67]. The successful fabrication of 3D ceramic-based material was also reported by other researchers [60,63]. In addition, FDM was also reported to produce inversely printed 3D bone grafts. In this technique, lead structures from PLA were printed with FDM for directional bone growth, filled with β -TCP slurry, and then burnt [62]. The compressive strength of the grafts was reported as 3.4 ± 0.2 MPa for 500 μ m spacing and reduced when incubated in simulated body fluids [62]. *In vitro* assays also showed that bone cells were able to adhere and proliferate in the grafts [62]. Given the benefits and the current success of FDM, it is predicted that the application of this method in generating 3D ceramic bone grafts will continue in the coming years.

4.1.3. Layer-by-layer 3D bioprinting method

Increasing demand for tissue/organ transplantation making the additive manufacturing technology for biological materials improved in recent years [52]. 3D bioprinting is one method that prints 3D parts containing biological material to mimic human tissue/organs [68]. The material that is being printed is called 'bioink' which is usually a combination of living cells, biomaterials, or active biomolecules [68]. Based on the method used, 3D bioprinting can be classified as either inkjet, extrusion, or laser-based bioprinting [52,68].

Inkjet, also called droplet bioprinting, was the first printing method that progressed from 2D to 3D and bioprinting. The printer in this method prints ink in droplets on the surface and forms a layer over time [52,69]. In designing a method for inkjet bioprinting, printing conditions should be taken carefully since this may alter culture conditions, especially the pH and temperature. A study by Firaldo *et al.* [70] used microwave-inkjet bioprinting with mesenchymal stem cells (MSCs) and collagen-based bio-ink to develop a cellularized human meniscus. The authors reported that only about 50% of the cells survived after 5 days of printing. However, after 28 days, the cells were able to grow and colonize in the graft [70]. Cell encapsulation in collagen gels, where the fiber network traps cells, is a common tissue engineering technique. Collagen gel pore size may be modified based on concentration for different uses and cell types [70]. However, bioprinting also can be performed without cell encapsulation. Gao *et al.* [71] used inkjet bioprinting to fabricate a 3D graft using poly(ethylene glycol) dimethacrylate, gelatin methacrylate, and human MSCs (hMSCs), in order to mimic bone and cartilage tissue. The fabrication was successful with more than 80% of the cells surviving during the printing process without extra steps for cell encapsulation. Graft also showed excellent osteogenic and chondrogenic differentiation capacity [71].

Another method that has also been used in 3D bioprinting technology is the extrusion bioprinting. Extrusion is the process of pushing extrusion-based material through a nozzle using an external source such as air pressure, a piston, or a screw [52]. The printing cost for this method is usually categorized as medium and has a low precision of printed parts [72]. Kang *et al.* [73] used extrusion-based technology to

fabricate a microchannel networks-enriched 3D hybrid scaffold composed of decellularized extracellular matrix, gelatin, chitosan, and nano-hydroxyapatite (nHA). The scaffold was extruded with pre-gel filaments at 20°C–25°C, crosslinked, frozen at –80°C, lyophilized, and combined with human adipose-derived stem cells (ADSCs) exosomes [73]. Authors reported that the addition of nHA improved the antibacterial properties of the scaffold, while the addition of exosomes promoted cell attachment and proliferation, as well as osteogenesis and vascularity regeneration *in vitro* and *in vivo* [73]. Other than gelatin and chitosan, collagen is one of the popular materials used in bioprinting technology due to its high affinity for cells adherent [74]. However, a lack of printability and low mechanical strength hampered collagen applicability through 3D bioprinting. This can be solved by altering the properties of the collagen bioink, for example by the addition of ceramic. It was proved that the addition of HA increased the strength of the scaffold, with BMSCs on the scaffold kept living and proliferating on the scaffold [75]. To archive a specific graft property, bioink also can be varied and combined. For instance, a study by Shen *et al.* [74] used extrusion-based technology to develop a bone tissue-engineering scaffold. The authors used two types of bio-ink; one is a photo-crosslinked extracellular matrix hydrogel supplemented with MSCs for osteogenesis, and the other is a templating bioink which is a thermosensitive hydrogel supplemented with endothelial cells (ECs) for angiogenesis [74]. This technique aims to enable ECs to form *in situ* vascular networks within a bone tissue-engineering scaffold [74]. The results showed that a coupling effect between angiogenesis and osteogenesis was archived *in vitro*, and also excellent performance in bone formation *in vivo* [74].

Other than inkjet and extrusion-based bioprinting, one printing technology that has been used to print biological material is laser-assisted bioprinting. Similar to SLA, laser-assisted bioprinting uses photopolymerization to create 3D structures with high printing resolution. Like the two existing bioprinting methods, collagen-based bioink is the most commonly used in laser-assisted bioprinting. However, other types of bioink also starting to be developed. Touya *et al.* [76] developed tricalcium silicate-based ink for laser-assisted bioprinting. The developed bioink confirmed all aspects of the formulation including rheological impact. Besides, the bioink also had great cytocompatibility, influencing cell motility and osteogenic differentiation response *in vitro*, promoting bone formation *in vivo*, and can deliver active compounds [76]. Laser-assisted bioprinting method is costly but offers rapid and high-resolution prototype technologies that allow for the exact organization of biomaterials in a predetermined configuration, which is suitable for *in situ* bioprinting [72,76–78]. Another study used laser-assisted bioprinting to organize endothelial cells in a mouse calvaria bone defect filled with collagen-containing MSCs and vascular endothelial growth factor. The *in situ* bioprinting was successful; defined local cell density and printing parameters allowed the generation of microvascular networks, which resulted in vascularization and bone regeneration into critical bone defects after two months *in vivo* [77]. A similar result was also reported by Kerequel *et al.* [78]. The authors utilized the laser-assisted

method for *in situ* bioprinting by using bioink that contained MSCs, collagen, and nHA for bone regeneration. Results showed that MSCs used in the study remained viable and proliferated *in vitro* and *in vivo* [78]. This proved that laser-assisted bioprinting method is a great approach for *in situ* bioprinting and tissue engineering.

In this review, no included articles used the 3D bioprinting method. This is due to the challenges of the graft characteristics when fabricated by the bioprinting method. The mechanical properties of grafts produced with bioprinting are commonly lower compared to grafts produced by other methods. For instance, the compressive strength of HA bone grafts made by the FDM method was reported to reach ~40 MPa due to the combination with a thermoplastic material [67], while the compressive strength of nHA bone graft by 3D bioprinting was about 7 to 16 MPa [73]. This issue makes the 3D bioprinted bone graft have difficulty adapting to the unique mechanical environment of load-bearing bones, which limits their potential applications [79]. In this study, we also detailed the utilization of these 3D printing methods, the materials used, and their characteristics in Table 5.

4.2. Materials used for 3D printed bone graft

Before being used in medical applications, the 3D bone grafts must first be designed to meet existing demands. Mechanical strength, elasticity, interconnected pores, and topography of the bone graft are important considerations for supporting bone healing in defective tissue [52,105]. These properties can only be achieved by selecting suitable materials, besides the 3D printing methods. We discussed in detail the characteristics of the ceramics and polymeric materials commonly used to fabricate 3D bone grafts, and also their impact on the properties of 3D printed bone grafts.

4.2.1. Ceramic material

Ceramics are commonly used in bone graft fabrication due to their inertness and biocompatibility. Tricalcium phosphate (TCP) and hydroxyapatite (HA) are the most used ceramics that are utilized as dental and orthopedic implants. TCP is a calcium salt of phosphoric acid, also known as tribasic calcium phosphate and bone phosphate of lime, with the chemical formula $\text{Ca}_3(\text{PO}_4)_2$. TCP has three polymorphs which are β -TCP, α -, and α' -TCP. β -TCP is the polymorph that is stable at room temperature and at 1125°C transforms to α -TCP and can be preserved after cooling to room temperature [12]. α -TCP is known to degrade more rapidly than β -TCP; α -TCP block began to degrade in the fourth week, while β -TCP in the eighth week when applied as augmenting highly resorbed alveolar ridges in rabbits [106]. This rapid degradation rate of α -TCP is due to the high solubility of α -TCP compared to β -TCP [107]. β -TCP is widely used as a mono- or biphasic bioceramic and bone graft composite [11,12], which is also used in the included studies of this review [14,108–113]. This is because the solubility of β -TCP is close to that of bone minerals, and as a result, can be resorbed by osteoclasts [11]. On the other hand, α -TCP is used as hydraulic bone cement due to its high solubility, hydration reaction, and bioresorbability [12,107].

Table 5. Outlined of ceramics material, 3D fabrication method, and characteristics of produced graft.

Type of Ceramics	Characteristics									
	Methods	Ceramics percentage	Additional Materials	Material's Strength	Elasticity	Biodegradability	Porosity	Pore Size	Contact Angle	Ref
nHA	FDM	30 and 50 wt%	PLLA (fiber preloaded with ceramics)	29.68 MPa (30 nHA wt%), 14.22 MPa (50 nHA wt%)	NA	11% (30 nHA wt %) and 15% (50 nHA wt%) mass degraded after 12 days	60%	NA	87.2° (30 nHA wt%), 77.4° (50 nHA wt %)	[80]
nHA	FDM	10, 20, 30, 40, and 50 wt%	PLA	~15–30 MPa (positively correlated with ceramic content)	NA	Fully degraded at day 17	~50–60%	NA	NA	[81]
nHA	FDM	10–20 wt%	PCL	4.5–8.67 MPa	3.83–8.51 MPa	NA	85.1% (10 wt%), 70.1% (20 wt%)	6.92 (10 wt%), 15.6 (20 wt%)	NA	[82]
HA	FDM	5, 10, 25, 20, 25 wt%	PCL	9 MPa (5 wt%) and 11 MPa (10 wt%)	24 to 30 Gpa	NA	60.0–65.4%	~550 µm	67° (25 wt%) to 87.8° (5 wt%)	[83]
nHA and mHA (each)	FDM	20 wt%	PCL	23.29 MPa for nHA and 20.25 for mHA MPa (tensile strength)	NA	NA	65.27% (nHA), 63.28% (mHA)	Length 239 µm and width 204 µm (nHA), length 217 µm and width 190 µm (mHA)	NA	[84]
nHA (biogenic)	FDM	15 wt%	PCL	NA	316 MPa (cuttlebone HA), 219 MPa (mussel HA), 203 MPa (eggshell HA)	NA	NA	328 µm (cuttlebone HA), 422 µm (mussel HA), 461 µm (eggshell HA)	NA	[85]
HA	FFF with ultrasonic vibration assistance	10 and 20 wt%	PLA	143.98–173.03 MPa (90 W ultrasonic vibration power)	NA	NA	NA	NA	NA	[86]
HA	FFF	15 wt%	PLA, polyhydroxyalkanoates, poly(3-hydroxybutyrate), magnesium	4.09–39.75 MPa (tensile strength)	31.86–119.31 MPa (Young's modulus)	NA	6.25–6.80%	0.8 mm	27.10–56.94°	[87]
HA (bovine)	SLA	5, 10, 20 wt%	Ceramic resin (slurries), silica	45 MPa for 5 wt% and 68 MPa for 10 wt % (compressive strength), 36 GPa for 5 wt% and 52 GPa for 10 wt%	20 MPa for 5 wt% and 40 MPa for 10 wt% (flexural strength)	NA	NA	NA	NA	[88]
HA and TCP	SLA	HA:TCP (6:4)	Acrylic monomers, photo initiator	2.80 MPa	NA	NA	NA	NA	NA	[89]
HA	SLA	NA	Photocurable binder matrix	~1.60 MPa	~513 MPa (elastic modulus)	NA	81.8%	≤1 µm and increased with CS content increase	NA	[90]
β-TCP	FDM	15 vol%	PLA	54.344–69.711 MPa (tensile strength)	1.685–2.161 GPa (Young's modulus)	NA	NA	NA	NA	[91]
β-TCP	FDM	10 wt%	PCL, PLGA	10.3–15.7 N (maximum tensile load)	594.7–803.0 (elastic modulus)	NA	~40%	200 µm	NA	[92]

(Continued)

Table 5. (Continued).

		Characteristics									
Type of Ceramics	Methods	Ceramics percentage	Additional Materials	Material's Strength	Elasticity	Biodegradability	Porosity	Pore Size	Contact Angle	Ref	
β -TCP and calcium sulfate	FDM	10, 15, 20 wt%	PCL	NA	NA	NA	50.92 (20% each), 43.96 (15% each), 54.12 (each 10%)	400–500 μ m	120.3° (20% each of β -TCP and calcium sulfate)	[93]	
β -TCP Calcium silicate (CS) and β -TCP	SLA SLA	50 wt% 0, 20, 40, 60, 80, 100 wt% (CS wt% to β -TCP)	Poly(D, L)-lactide NA	13 MPa–23 MPa (0.5 W laser power) Decreased when CS content increase	NA NA	NA CS 100 wt% lost the least weight in 30 days compared to CS 0 wt%	Increased with CS content increase	NA \leq 1 μ m and increased with CS content increase	NA NA	[94] [95]	
β -TCP	Liquid crystal display	10, 20, 30, 35 wt%	PLA	50 MPa (10 wt%), 48 MPa (20 wt%), 25 MPa (30 wt%), 10 MPa (35 wt%)	NA	10.5% (10 wt%), 11.5% (20 wt%), 12.5% (30 wt%), 12.97% (35 wt%)	48.3% (10 wt%), 45.9% (20 wt%), 43.6% (30 wt%), 40.4% (35 wt%)	NA	NA	[96]	
β -TCP	SLS	NA	PCL or alendronate (coated)	5.74 MPa (uncoated PCL), 5.58 MPa (PCL coated)	NA	NA	NA	311 μ m	NA	[97]	
Calcium phosphate powders (HA, β -TCP, BCP)	Inkjet	NA	Polyvinyl butyral, polyvinyl alcohol, polyethylene glycol	5.5 Mpa (60% porosity), 3.0 Mpa (70% porosity), 1.0 Mpa (80% porosity)	NA	NA	50% (pore size 200 μ m), 75% (pore size 700 μ m)	200 μ m, 400 μ m, 700 μ m	NA	[98]	
Bioglass BGS-7	FDM	20, 40, 60 wt%	PCL	2.5–2.9 Nmm ⁻¹ (60 wt%) (increased as the bioglass content increase)	4.3–6.3 MPa (bending stress max, decreased as the bioglass content increase)	NA	42.3–43.1	~200 μ m	Decreased with the increase of BGS content	[99]	
Bioactive glass	FDM	5, 10, 20 wt%	PCL	36.75–43.52 MPa (compressive strength, increased as the bioglass content increase), 4.63–5.82 MPa (20% tensile strength, decreased as the bioglass content increase)	NA	NA	45.70–48.10%	372.3 μ m	87.99–116.04° (decreased as the bioglass content increase)	[100]	
Bioactive glass 635	FDM	5, 10, 20 wt%	PCL	NA	4.79977 N/mm ² (highest elastic modulus)	22.5–45% (increased as the bioglass content increase)	~50%	NA	82.85–86.75°	[101]	
Bioactive glass 4555	FDM	10, 15, 20 wt%	PCL	~270–340 MPa (compressive modulus), ~8.5–11 MPa (0.2% offset yield strength)	NA	10.61–20.68 (increased as the bioglass content increase)	~52%	264–330 μ m (internal region)	~50–69°	[102]	
Bioglass S53P4	FFF	5%, 10%, 20 wt%	PLA	100–180 Mpa	NA	NA	NA	180 μ m–2 mm	NA	[103]	
Bioactive glass 13–93	SLS	50, 60 wt%	Polymeric binder	5.9–20.4 Mpa	NA	NA	58.8%	300–800 μ m	NA	[104]	

NA, not available.

One article in the included studies used hydroxyapatite (HA) as ceramic material in the 3D printed graft [7]. HA is the most stable of all calcium orthophosphates with the chemical formula of $\text{Ca}_{10}(\text{PO}_4)_6(\text{OH})_2$ [12]. HA is a widely used biomaterial in the orthopedic and dental fields. As a biomaterial, HA is known to have biocompatible, biodegradable, osteoconductive, and osteoinductive properties due to their inertness in chemical and physical features with bone inorganic components [13,114,115].

Although both are calcium phosphate derivatives and extensively utilized as biomaterials, β -TCP and HA have different properties that may influence the selection of these ceramics for bone graft fabrication. HA is substantially more crystalline than bone mineral, making HA-based implants chemically more stable and consequently non-degradable upon implantation [11,21]. This makes HA degrade more slowly and less resorbable compared to TCP [21]. Because of this property, HA is usually used as a scaffold for bone ingrowth, giving a stable framework for calcification to occur in place [116]. Due to its osteoinductivity, HA is also been used as a coating material in metal and ceramic-based bone grafts, including TCP [117]. HA coating in β -TCP porous graft greatly increased alkaline phosphatase and bone sialoprotein levels in preosteoblasts [117].

Several factors in the synthesis process can alter the solubility, reactivity, bioresorbability, and behavior in the biological environments of the ceramics. Metal ions including Sr^{2+} , Zn^{2+} , and Mg^{2+} change the stability of α - and β - phases by replacing Ca^{2+} ions in the TCP lattice, which stabilizes the β -TCP phase [107]. In HA, cation doping was reported to alter particle size and adsorption capacity [118]. This doping is frequently an uncontrolled side consequence of elemental contaminants in the synthesis method. However, it can also be employed in a controlled setting to alter biological features [11]. Continuously released Zn^{2+} and Ca^{2+} from doped-PLGA/ β -TCP graft made by 3D exhibited higher osteogenic and anti-inflammatory properties compared to PLGA/ β -TCP graft alone [119], which is also in line with other reports [120,121]. However, the commercial success of ion-doped ceramic for medical applications is still undetectable due to the regulatory burden in commercialization [11].

TCP and HA are widely used as 3D-printed bone grafts together with polymeric material. It has been proved that they can induce new bone growth and have biodegradable properties [7,122]. However, the use of HA and β -TCP and its combination with polymeric material as a 3D-printed bone graft must be carefully considered by the surgeon and depends on the needs of the patient. Ceramic 3D-printed bone graft is not suitable for conditions that require permanent replacement of bone tissue considering that most of the material in the graft is biodegradable.

4.2.2. Synthetic polymeric material

Ceramics such as TCPs and HA, however, have brittle character [11,15]. Because of this, the use of ceramic as a single material in bone regeneration is not effective, especially for load-bearing applications [11]. Most ceramics are formulated with

other materials for application as bone scaffolds. For 3D printing fabrication, synthetic polymers have been widely used to improve bone grafts' mechanical properties. In 3D printing, ceramic can be combined with polymers to up to 30% to meet the mechanical requirement, osteogenesis, and prevent needle clogging [123]. These are polycaprolactone (PCL), polylactic acid (PLA), polyglycolic acid (PGA), polylactic-co-glycolide (PLGA), poly(methyl methacrylate) (PMMA), polyethylene (PE), and polyetheretherketone (PEEK) [18]. Among them, PCL and PLA are the most used synthetic polymers for 3D printing applications [17,18].

It should be emphasized that the compressive strength of trabecular bone varies substantially with anatomical location and individual parameters such as bone density [124]. As a result, the use of bioceramic scaffolds must be tailored to the strength of the bones they will support. The addition of ceramic to PLA/PCL-based bone grafts has been reported to significantly alter the mechanical strength of the grafts. Nyberg *et al.* [60] reported that the addition of TCP did not change the compressive modulus of the PCL graft. However, the addition of HA significantly increased the compressive modulus in the solid and porous form of the grafts [60]. HA also was reported to increase the stiffness of the PCL-based graft [125]. These findings explained that HA has strong interactions with the PLA/PCL matrix, which transfers the load effectively between the ceramic and polymer in both compression and tensile tests. On another hand, Wang *et al.* [67] showed that the addition of nanosized β -TCP increased the roughness and surface hydrophilicity, but lowered the mechanical strength of the PLA-based grafts. Another study also reported similar results with the PCL-based bone grafts [63]. The study showed the addition of TCP to 60% decreased the yield strength of the PCL-based filaments, this was also proportional and inversely proportional to the grafts' surface roughness and contact angle [63]. Nevertheless, the slight decrease in strength did not affect the performance of the grafts which was proven by the superior osteogenic ability and bone repair capacity of the bone grafts [63,67]. However, additional considerations are required, notably adjustments to the architecture and character of the injured bone to ensure the stability of bone graft fixation, especially in situations with critical-sized bone defects.

PLA is a biodegradable thermoplastic, semi-crystalline polymer with a slow rate of crystallization that comes from renewable resources such as corn starch and sugarcane [18]. A previous systematic review explored the use of PLA/ceramics bone grafts in animal studies [17]. The author outlined the biocompatible and mechanically resistant character of PLA/ceramics-based bone grafts have promising applications in clinical cases [17]. However, our review showed that there are no human studies that used PLA/ceramics material, yet, PCL/ceramics 3D composite [14,110–113,126]. This shift in thermoplastic polymer selection in animal and human studies is suggested due to the character preference of the polymer. PLA and PCL differ in physical and mechanical properties. In comparison, the density of PLA and PCL are 1.21–1.25 g/cm³ and 1.11–1.14 g/cm³, the glass transition temperature of PLA and PCL are 45–60°C and (–60)–(–65) °C, and the melting

temperatures of PLA and PCL are 150–162°C and 58–65°C, respectively [18,19]. PLA is more brittle compared to PCL [18]. Important notes that PLA may cause an inflammatory response in the host [18]. This happens if the surrounding tissue can not eliminate the lactic acid produced from its breakdown results [127]. Moreover, PLA also presents hydrophobicity and low cell affinity which negatively affects the cells' adhesion to the PLA-based graft [17]. This biological effect might represent the reasons why PLA is not employed as a thermoplastic polymer in 3D printing applications for humans. Modifying the surface characteristic of PLA can provide beneficial surface properties while simultaneously minimizing the innate immune response by regulating cytokine production [17,20]. Nevertheless, further studies on this need to be conducted strictly, including in clinical settings.

4.3. Standardization and future perspective

Despite being a customized product, 3D bone grafts must be standardized before use for clinical applications. Standardization of 3D-printed materials must refer to the regulations of each country. However, the use of references such as ISO (International Organization for Standardization) can be considered. 3D-printed ceramic bone graft is a 'medical device' that is included in the implant group and can be used alone or in combination for human beings with exposure which is generally more than 30 days. Based on ISO 10993, physical and chemical information on materials that are in direct contact with patients must be obtained which makes materials characterization required. Chemical characterization by using ICP and XRD is required for ceramics-based medical devices. Biological evaluations must be carried out including cytotoxicity, haemocompatibility, implantation effects, and degradation test of the graft. Moreover, toxicokinetic studies that evaluate absorption, distribution, metabolism, and excretion should be considered if the medical devices are designed to be absorbable or to be in long-term contact with bone tissue [128]. Dental implants that contain ceramics should be tested in a low pH solution and *in vivo* pH solution to check the possible degradation product of the ceramics. On the other hand, degradation products from polymeric grafts can be examined by using the accelerated test, and if necessary real-time degradation test can be used [128]. Biocompatibility of the material can be defined first by using cytotoxicity assay using cell lines and can be done with extract, direct contact, or indirect contact with the graft. Testing for biocompatibility may include, but is not limited to sensitization, genotoxicity, implantation, chronic toxicity, and carcinogenicity [128].

Functional testing is required to make sure the manufactured graft can perform as intended in addition to tests to guarantee the graft's safety. As a bone support, for instance, the graft needs to be at least as strong as the cortical bone tissue it supports, especially in load-bearing districts. In comparison to maxillofacial-application grafts, higher mechanical strength is anticipated when the graft presents a weight-bearing intended use in the load-bearing districts, such as the femur, tibia, or spine. Ninarello *et al.* reviewed marked grafts for load-bearing applications and found that the orthopedic/spine group was almost 3.3 times higher than the mean

value for the oral/cranio-maxillofacial application group (22.4 MPa vs 6.8 MPa). Mechanical testing should also be based on a particular standard, for example referring to the materials used. ISO 13175-3:2012 can be used to characterize calcium phosphate grafts including HA, while grafts made from rigid plastic can be characterized following the procedure in ASTM D695-23 (2023) [129].

Furthermore, standardization of manufacturing techniques and the characteristics of the manufactured bone graft should be implemented (Figure 6). In the U.S.A., 3D-printed medical equipment is regulated by the FDA's Center for Medical Devices and Radiological Health (CDRH). However, in terms of the addition of biological components, it is required the additional involvement of the Center for Biologics Evaluation and Research (CBER) [130]. The FDA categorizes the additive manufacturing process of a medical device into five phases: Designing, software workflow, building, post-processing, and final testing consideration. In the designing process, patient CT or MRI data is transformed into a DICOM-compatible format. During the software workflow stage, an image segmentation system separates the anatomical region of interest from the rest of the scan. The file can be optimized further before being converted to a 3D printer-compatible format, such as standard triangulation language (STL). Then the build stage is the material selection stage. The selection stages must be adjusted to the patient's needs, especially regarding the condition of the defective tissue and its characteristics along with accompanying medical conditions in the existing patient. The operator must choose a suitable printing technique based on the materials and desired properties of the bone graft. In this review, we also outlined the 3D-printed bone graft fabrication methods, the materials used, and the characteristics of the fabricated grafts (Table 5). This may help manufacturers and/or surgeons in general in selecting materials and methods or products based on the needs of each patient.

Aside from that, post-processing is a stage that includes sterilization of the bone graft. To be FDA-cleared for intraoperative usage, all 3DMD must be validated at a certain sterility assurance level (SAL) [131]. The SAL is defined as the predicted likelihood of a live microbe after sterilization. The FDA specifies a SAL < 10⁻³ for devices that contact the skin and SAL < 10⁻⁶ for implanted devices [5,130,131]. Sterilization of bone grafts must still maintain their existing characteristics. For example, bone grafts with thermoplastic polymers should not be sterilized with high temperature, but the sterilization method may be different if the main material used is titanium [5,130,131]. Further, the device can then be characterized at the final testing consideration stage. This stage is to determine whether the bone graft's characteristics meet the desired requirements depending on the properties of the damaged tissue that will receive the bone graft [130]. In the end, the development process of the 3D-printed bone graft requires the collaboration of surgeons, manufacturers, biomedical engineers, and regulatory bodies.

This review has several shortcomings. First, we include all types of human studies since there are only limited clinical reports discussing 3D-printed ceramic bone grafts. The types of study can indirectly influence the outcomes reported in the

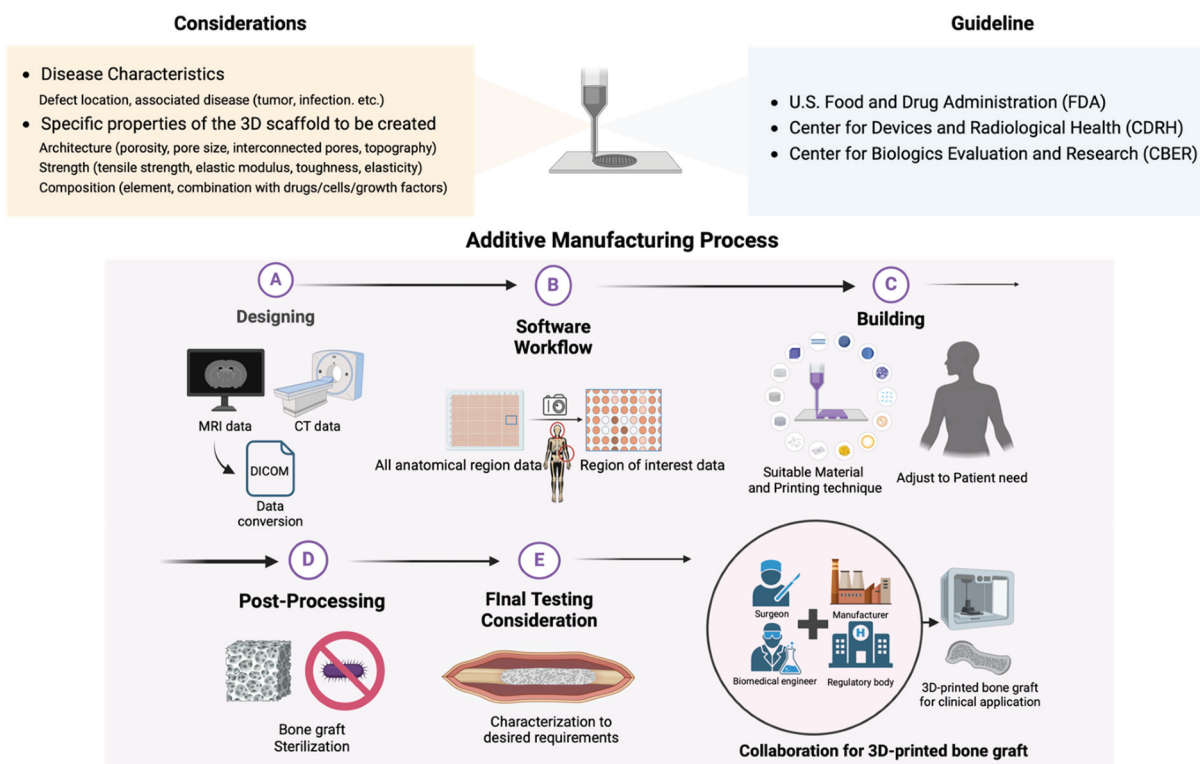


Figure 6. Work-flow and quality control of 3D-printed medical bone graft.

included articles and, thus, may influence the postoperative complication rate (CR%) reported in this review. Second, most of the reports only focus on existing outcomes, whereas how the bone graft is fabricated and its characteristics are difficult to track. Third, the identification of postoperative complications was also based on the decision of each surgeon in the included studies, and most of the studies did not report additional investigation if the complications were related to the bone graft or not. Fourth, in this study, we did not analyze the CR% based on the longevity use of the graft due to limited articles in the included studies and the limited information about this in each study. However, we believe that information about postoperative complications in the clinical uses of 3D-printed ceramic grafts, as well as comprehensive details about materials and fabrication methods, can provide valuable information for researchers in this field and help industry and clinicians to choose materials and fabrication processes for 3D-printed ceramic bone grafts.

5. Conclusion

Here we review in detail the outcomes of the use of ceramic-based 3D-printed bone grafts reported in humans. The proportional meta-analysis revealed that the total postoperative complication rate for 3D ceramic-based bone grafts was 14.3%. In this review, we also detailed the use of ceramic and synthetic polymers in customized bone grafts, as well as the methods used. We discovered that the presence of synthetic polymers, such as PLA/PCL, increases the mechanical strength of grafts and causes controlled graft breakdown. On the other hand, the effect of ceramic on the characteristics of

the composite depends on the nature of each ceramic. The addition of other materials, such as growth factors or cells, improves the bioactive and osteoinductive features of bone grafts and allows for tissue engineering applications. Similarly, standardization in bone graft production is critical, which includes material selection, production techniques, and the expected characteristics of the finished bone graft. This is inextricably linked to the patient's condition and the damaged tissue that will receive the bone graft.

Funding

This work is financially supported by program Hibah Dosen Tidak Tetap Peneliti 2024 managed by The Directorate for Multidisciplinary Science and Technology Implementation (DPITM), Institut Teknologi Bandung, financially from the DAPT EQUITY Program, Indonesia Endowment Fund for Education (LPDP), the Ministry of Finance, Indonesia. This work is also partially supported by the Asahi Glass Foundation (Overseas Research Grant 2024). The funders had no role in study design, data collection and analysis, decision to publish, or preparation of the manuscript.

Declaration of interest

The authors have no other relevant affiliations or financial involvement with any organization or entity with a financial interest in or financial conflict with the subject matter or materials discussed in the manuscript apart from those disclosed.

Reviewer disclosures

Peer reviewers on this manuscript have no relevant financial relationships or otherwise to disclose.

Author contributions

M.A.G contributed to the conceptualization, methodology, software, formal analysis, investigation, resources, data curation, writing – original draft, writing – review & editing, and funding acquisition. H.D.M contributed to the investigation, data curation, writing – review & editing. G.L contributed to the resources and visualization. S.F.R contributed to the writing – review & editing. P.D.A.A contributed to the writing – review & editing and project administration. T.S contributed to the project administration. R.L contributed to the validation and supervision. I.K.A contributed to the validation and supervision. K.L to the validation and supervision. D.B contributed to the methodology, validation, supervision, and funding acquisition. All authors have approved the most recent submitted version (and any substantially modified version that involves the author's contribution to the study); and agreed to be personally accountable for the author's own contributions and to ensure that questions related to the accuracy or integrity of any part of the work, even ones in which the author was not personally involved, are appropriately investigated, resolved, and the resolution documented in the literature.

References

- Stewart S, Bryant SJ, Ahn J, et al. Bone regeneration. In: *Translational Regenerative Medicine*. 2015. p. 313–333.
- Cheung WH, Miclau T, Chow SKH, et al. Fracture healing in osteoporotic bone. *Injury*. 2016;47:S21–S26. doi: [10.1016/S0020-1383\(16\)47004-X](https://doi.org/10.1016/S0020-1383(16)47004-X)
- Roddy E, DeBaun MR, Daoud-Gray A, et al. Treatment of critical-sized bone defects: clinical and tissue engineering perspectives. *Eur J Orthop Surg Traumatol*. 2018;28(3):351–362. doi: [10.1007/s00590-017-2063-0](https://doi.org/10.1007/s00590-017-2063-0)
- Schemitsch EH. Size matters: defining critical in bone defect size! *J Orthop Trauma*. 2017;31(5):S20–S22. doi: [10.1097/BOT.0000000000000978](https://doi.org/10.1097/BOT.0000000000000978)
- Paxton NC. Navigating the intersection of 3D printing, software regulation and quality control for point-of-care manufacturing of personalized anatomical models. *3D Print Med*. 2023;9(1):1–12. doi: [10.1186/s41205-023-00175-x](https://doi.org/10.1186/s41205-023-00175-x)
- Kanno Y, Nakatsuka T, Saijo H, et al. Computed tomographic evaluation of novel custom-made artificial bones, “CT-bone”, applied for maxillofacial reconstruction. *Regen Ther*. 2016;5:1–8. doi: [10.1016/j.reth.2016.05.002](https://doi.org/10.1016/j.reth.2016.05.002)
- Brie J, Chartier T, Chaput C, et al. A new custom made bioceramic implant for the repair of large and complex craniofacial bone defects. *J Cranio-Maxillofacial Surg*. 2013;41(5):403–407. doi: [10.1016/j.jcms.2012.11.005](https://doi.org/10.1016/j.jcms.2012.11.005)
- Dimitriou R, Mataliotakis GI, Angoules AG, et al. Complications following autologous bone graft harvesting from the iliac crest and using the RIA: a systematic review. *Injury*. 2011;42(SUPPL. 2):S3–S15. doi: [10.1016/j.injury.2011.06.015](https://doi.org/10.1016/j.injury.2011.06.015)
- Calori GM, Colombo M, Mazza EL, et al. Incidence of donor site morbidity following harvesting from iliac crest or RIA graft. *Injury*. 2014;45(S6):S116–S120. doi: [10.1016/j.injury.2014.10.034](https://doi.org/10.1016/j.injury.2014.10.034)
- Markets M and. 3D printing medical devices market. 2023.
- Bohner M, Santoni BLG, Döbelin N. β -tricalcium phosphate for bone substitution: synthesis and properties. *Acta Biomater*. 2020;113:23–41. doi: [10.1016/j.actbio.2020.06.022](https://doi.org/10.1016/j.actbio.2020.06.022)
- Carrodegua RG, De Aza S. α -tricalcium phosphate: synthesis, properties and biomedical applications. *Acta Biomater*. 2011;7(10):3536–3546. doi: [10.1016/j.actbio.2011.06.019](https://doi.org/10.1016/j.actbio.2011.06.019)
- Gani MA, Budiadin AS, Shinta DW, et al. Bovine hydroxyapatite-based scaffold accelerated the inflammatory phase and bone growth in rats with bone defect. *J Appl Biomater Funct Mater*. 2023;0(0):1–12. doi: [10.1177/22808000221149193](https://doi.org/10.1177/22808000221149193)
- Laubach M, Suresh S, Herath B, et al. Clinical translation of a patient-specific scaffold-guided bone regeneration concept in four cases with large long bone defects. *J Orthop Translat*. 2022;34(January):73–84. doi: [10.1016/j.jot.2022.04.004](https://doi.org/10.1016/j.jot.2022.04.004)
- Khotib J, Gani MA, Budiadin AS, et al. Signaling pathway and transcriptional regulation in osteoblasts during bone healing: direct involvement of hydroxyapatite as a biomaterial. *Pharmaceuticals*. 2021;14(7):615. doi: [10.3390/ph14070615](https://doi.org/10.3390/ph14070615)
- Fortelny I, Ujčić A, Fambri L, et al. Phase structure, compatibility, and toughness of PLA/PCL blends: a review. *Front Mater*. 2019;6(August):1–13. doi: [10.3389/fmats.2019.00206](https://doi.org/10.3389/fmats.2019.00206)
- Alonso-Fernández I, Haugen HJ, López-Peña M, et al. Use of 3D-printed polylactic acid/bioceramic composite scaffolds for bone tissue engineering in preclinical in vivo studies: a systematic review. *Acta Biomater*. 2023;168:1–21. doi: [10.1016/j.actbio.2023.07.013](https://doi.org/10.1016/j.actbio.2023.07.013)
- Alizadeh-Osgouei M, Li Y, Wen C. A comprehensive review of biodegradable synthetic polymer-ceramic composites and their manufacture for biomedical applications. *Bioact Mater*. 2019;4(1):22–36. doi: [10.1016/j.bioactmat.2018.11.003](https://doi.org/10.1016/j.bioactmat.2018.11.003)
- Van de Velde K, Kiekens P. Biopolymers: overview of several properties and consequences on their applications. *Polym Test*. 2002;21(4):433–442. doi: [10.1016/S0142-9418\(01\)00107-6](https://doi.org/10.1016/S0142-9418(01)00107-6)
- Stankevich KS, Gudima A, Filimonov VD, et al. Surface modification of biomaterials based on high-molecular polylactic acid and their effect on inflammatory reactions of primary human monocyte-derived macrophages: perspective for personalized therapy. *Mater Sci Eng C*. 2015;51:117–126. doi: [10.1016/j.msec.2015.02.047](https://doi.org/10.1016/j.msec.2015.02.047)
- Shimazaki K, Mooney V. Comparative study of porous hydroxyapatite and tricalcium phosphate as bone substitute. *J Orthop Res*. 1985;3(3):301–310. doi: [10.1002/jor.1100030306](https://doi.org/10.1002/jor.1100030306)
- Sotome S, Ae K, Okawa A, et al. Efficacy and safety of porous hydroxyapatite/type 1 collagen composite implantation for bone regeneration: a randomized controlled study. *J Orthop Sci*. 2016;21(3):373–380. doi: [10.1016/j.jos.2016.01.007](https://doi.org/10.1016/j.jos.2016.01.007)
- McKenna GJ, Gjengedal H, Harkin J, et al. Effect of autogenous bone graft site on dental implant survival and donor site complications: a systematic review and meta-analysis. *J Evidence-Based Dent Pract*. 2022;22(3):101731. doi: [10.1016/j.jebdp.2022.101731](https://doi.org/10.1016/j.jebdp.2022.101731)
- Yoon B-H, Park IK, Kim Y, et al. Incidence of nonunion after surgery of distal femoral fractures using contemporary fixation device: a meta-analysis. *Arch Orthop Trauma Surg*. 2021;141(2):225–233. doi: [10.1007/s00402-020-03463-x](https://doi.org/10.1007/s00402-020-03463-x)
- Moher D, Shamseer L, Clarke M, et al. Preferred reporting items for systematic review and meta-analysis protocols (PRISMA-P) 2015 statement. *Syst Rev*. 2015;4(1):1. doi: [10.1186/2046-4053-4-1](https://doi.org/10.1186/2046-4053-4-1)
- Moher D, Liberati A, Tetzlaff J, et al. Preferred reporting items for systematic reviews and meta-analyses: the PRISMA statement. *PLoS Med*. 2009;6(7):e1000097. doi: [10.1371/journal.pmed.1000097](https://doi.org/10.1371/journal.pmed.1000097)
- Mandelli F, Traini T, Ghensi P. Customized-3D zirconia barriers for guided bone regeneration (GBR): clinical and histological findings from a proof-of-concept case series. *J Dent*. 2021;114(April):103780. doi: [10.1016/j.jdent.2021.103780](https://doi.org/10.1016/j.jdent.2021.103780)
- Mangano F, Zecca P, Pozzi-Taubert S, et al. Maxillary sinus augmentation using computer-aided design/computer-aided manufacturing (CAD/CAM) technology. *Int J Med Robot Comput Assisted Surg*. 2013;9(3):331–338. doi: [10.1002/rcs.1460](https://doi.org/10.1002/rcs.1460)
- Marcacci M, Kon E, Moukhachev V, et al. Stem cells associated with macroporous bioceramics for long bone repair: 6- to 7-year outcome of a pilot clinical study. *Tissue Eng*. 2007;13(5):947–955. doi: [10.1089/ten.2006.0271](https://doi.org/10.1089/ten.2006.0271)
- Morrison DA, Kop AM, Nilasaroya A, et al. Cranial reconstruction using allogeneic mesenchymal stromal cells: a phase 1 first-in-human trial. *J Tissue Eng Regen Med*. 2018;12(2):341–348. doi: [10.1002/term.2459](https://doi.org/10.1002/term.2459)
- Nickenig H-J, Riekert M, Zirk M, et al. 3D-based buccal augmentation for ideal prosthetic implant alignment—an optimized method and report on 7 cases with pronounced buccal concavities. *Clin Oral Investig*. 2022;26(5):3999–4010. doi: [10.1007/s00784-022-04369-1](https://doi.org/10.1007/s00784-022-04369-1)
- Wolff J, Sándor G, Miettinen A, et al. GMP-level adipose stem cells combined with computer-aided manufacturing to reconstruct mandibular ameloblastoma resection defects: experience with three cases. *Ann Maxillofac Surg*. 2013;3(2):114. doi: [10.4103/2231-0746.119216](https://doi.org/10.4103/2231-0746.119216)

33. Yang H, Fang X, Xiong Y, et al. 3D customized biological tibial intramedullary nail fixation for the treatment of fracture after massive allograft bone transplantation of tibial osteosarcoma: a case report. *Orthop Surg.* 2022;14(6):1241–1250. doi: [10.1111/os.13294](https://doi.org/10.1111/os.13294)
34. Sprio S, Fricia M, Maddalena GF, et al. Osteointegration in cranial bone reconstruction: a goal to achieve. *J Appl Biomater Funct Mater.* 2016;14(4):470–476. doi: [10.5301/jabfm.5000293](https://doi.org/10.5301/jabfm.5000293)
35. Lu J, Wang QY, Sheng JG, et al. A 3D-printed, personalized, biomechanics-specific beta-tricalcium phosphate bioceramic rod system: personalized treatment strategy for patients with femoral shaft non-union based on finite element analysis. *BMC Musculoskelet Disord.* 2020;21(1):1–9. doi: [10.1186/s12891-020-03465-1](https://doi.org/10.1186/s12891-020-03465-1)
36. Mangano C, Giuliani A, De Tullio I, et al. Case report: histological and histomorphometrical results of a 3-D printed biphasic calcium phosphate ceramic 7 years after insertion in a human maxillary alveolar ridge. *Front Bioeng Biotechnol.* 2021;9(April):1–9. doi: [10.3389/fbioe.2021.614325](https://doi.org/10.3389/fbioe.2021.614325)
37. Munn Z, Barker TH, Moola S, et al. Methodological quality of case series studies: an introduction to the JBI critical appraisal tool. *JBI Database System Rev Implement Rep.* 2019; Publish Ahead of Print:2127–2133. doi: [10.11124/JBISRIR-D-19-00099](https://doi.org/10.11124/JBISRIR-D-19-00099)
38. Zeng X, Zhang Y, Kwong JSW, et al. The methodological quality assessment tools for preclinical and clinical studies, systematic review and meta-analysis, and clinical practice guideline: a systematic review. *J Evid Based Med.* 2015;8(1):2–10. doi: [10.1111/jebm.12141](https://doi.org/10.1111/jebm.12141)
39. Bloom O, Goddard N, Yannoulis B, et al. The successful use of a bespoke OssDsign cranial plate to reconstruct an occipital defect following excision of a recurrent epithelioid sarcoma. *JPRAS Open.* 2020;24(July 2019):71–76. doi: [10.1016/j.jp.2020.01.002](https://doi.org/10.1016/j.jp.2020.01.002)
40. Lee UL, Lim JY, Park SN, et al. A clinical trial to evaluate the efficacy and safety of 3d printed bioceramic implants for the reconstruction of zygomatic bone defects. *Materials.* 2020;13(20):1–13. doi: [10.3390/ma13204515](https://doi.org/10.3390/ma13204515)
41. Mangano F, Macchi A, Shibli JA, et al. Maxillary ridge augmentation with custom-made CAD/CAM scaffolds. A 1-year prospective study on 10 patients. *J Oral Implantology.* 2014;40(5):561–569. doi: [10.1563/AAID-JOI-D-12-00122](https://doi.org/10.1563/AAID-JOI-D-12-00122)
42. Mangano FG, Zecca PA, Van Noort R, et al. Custom-made computer-aided-design/computer-aided-manufacturing biphasic calcium-phosphate scaffold for augmentation of an atrophic mandibular anterior ridge. *Case Rep Dent.* 2015;2015:1–11. doi: [10.1155/2015/941265](https://doi.org/10.1155/2015/941265)
43. Figliuzzi M, Mangano FG, Fortunato L, et al. Vertical ridge augmentation of the atrophic posterior mandible with custom-made, computer-aided design/computer-aided manufacturing porous hydroxyapatite scaffolds. *J Craniofacial Surg.* 2013;24(3):856–859. doi: [10.1097/SCS.0b013e31827ca3a7](https://doi.org/10.1097/SCS.0b013e31827ca3a7)
44. Staffa G, Nataloni A, Compagnone C, et al. Custom made cranio-plasty prostheses in porous hydroxy-apatite using 3D design techniques: 7 years experience in 25 patients. *Acta Neurochir (Wien).* 2007;149(2):161–170. doi: [10.1007/s00701-006-1078-9](https://doi.org/10.1007/s00701-006-1078-9)
45. Staffa G, Barbanera A, Faiola A, et al. Custom made bioceramic implants in complex and large cranial reconstruction: a two-year follow-up. *J Cranio-Maxillofacial Surg.* 2012;40(3):e65–e70. doi: [10.1016/j.jcms.2011.04.014](https://doi.org/10.1016/j.jcms.2011.04.014)
46. Hardy H, Tollard E, Derrey S, et al. Tolérance clinique et degré d'ossification des cranioplasties en hydroxyapatite de larges défauts osseux. *Neurochirurgie.* 2012;58(1):25–29. doi: [10.1016/j.neuchi.2011.09.006](https://doi.org/10.1016/j.neuchi.2011.09.006)
47. Schaefer O, Kuepper H, Thompson GA, et al. Effect of CNC-milling on the marginal and internal fit of dental ceramics: a pilot study. *Dent Mater.* 2013;29(8):851–858. doi: [10.1016/j.dental.2013.04.018](https://doi.org/10.1016/j.dental.2013.04.018)
48. Trunec M, Chlup Z. Subtractive manufacturing of customized hydroxyapatite scaffolds for bone regeneration. *Ceram Int.* 2017;43(14):11265–11273. doi: [10.1016/j.ceramint.2017.05.177](https://doi.org/10.1016/j.ceramint.2017.05.177)
49. Fabris D, Mesquita-Guimarães J, Pinto P, et al. Mechanical properties of zirconia periodic open cellular structures. *Ceram Int.* 2019;45(13):15799–15806. doi: [10.1016/j.ceramint.2019.05.010](https://doi.org/10.1016/j.ceramint.2019.05.010)
50. Zhang X, Yu T, Li M, et al. Effect of machining parameters on the milling process of 2.5D C/SiC ceramic matrix composites. *Machining Sci Technol.* 2020;24(2):227–244. doi: [10.1080/10910344.2019.1636271](https://doi.org/10.1080/10910344.2019.1636271)
51. Zhang Q, Zhou J, Zhi P, et al. 3D printing method for bone tissue engineering scaffold. *Med Nov Technol Devices.* 2023;17(December 2022):100205. doi: [10.1016/j.medntd.2022.100205](https://doi.org/10.1016/j.medntd.2022.100205)
52. Thangavel M, Elsen Selvam R. Review of physical, mechanical, and biological characteristics of 3D-Printed bioceramic scaffolds for bone tissue engineering applications. *ACS Biomater Sci Eng.* 2022;8(12):5060–5093. doi: [10.1021/acsbomaterials.2c00793](https://doi.org/10.1021/acsbomaterials.2c00793)
53. Sodeyama MK, Ikeda H, Nagamatsu Y, et al. Printable PICN composite mechanically compatible with human teeth. *J Dent Res.* 2021;100(13):1475–1481. doi: [10.1177/00220345211012930](https://doi.org/10.1177/00220345211012930)
54. Hann SY, Cui H, Esworthy T, et al. Dual 3D printing for vascularized bone tissue regeneration. *Acta Biomater.* 2021;123:263–274. doi: [10.1016/j.actbio.2021.01.012](https://doi.org/10.1016/j.actbio.2021.01.012)
55. Wiria FE, Leong KF, Chua CK, et al. Poly-ε-caprolactone/hydroxyapatite for tissue engineering scaffold fabrication via selective laser sintering. *Acta Biomater.* 2007;3(1):1–12. doi: [10.1016/j.actbio.2006.07.008](https://doi.org/10.1016/j.actbio.2006.07.008)
56. Rahmani R, Molan K, Brojan M, et al. High virucidal potential of novel ceramic-metal composites fabricated via hybrid selective laser melting and spark plasma sintering routes. *Int J Adv Manuf Technol.* 2022;120(1–2):975–988. doi: [10.1007/s00170-022-08878-x](https://doi.org/10.1007/s00170-022-08878-x)
57. Wang D, Wang Y, Wu S, et al. Customized a Ti6Al4V bone plate for complex pelvic fracture by selective laser melting. *Materials.* 2017;10(1):1–14. doi: [10.3390/ma10010001](https://doi.org/10.3390/ma10010001)
58. Guo Y, Xie K, Jiang W, et al. In vitro and in vivo study of 3D-Printed porous tantalum scaffolds for repairing bone defects. *ACS Biomater Sci Eng.* 2019;5(2):1123–1133. doi: [10.1021/acsbomaterials.8b01094](https://doi.org/10.1021/acsbomaterials.8b01094)
59. Park JH, Tucker SJ, Yoon J, et al. 3D printing modality effect: distinct printing outcomes dependent on selective laser sintering (SLS) and melt extrusion. *J Biomed Mater Res A.* 2024;112(7):1015–1024. doi: [10.1002/jbm.a.37682](https://doi.org/10.1002/jbm.a.37682)
60. Nyberg E, Rindone A, Dorafshar A, et al. Comparison of 3D-Printed poly-ε-caprolactone scaffolds functionalized with tricalcium phosphate, hydroxyapatite, bio-oss, or decellularized bone matrix. *Tissue Eng Part A.* 2017;23(11–12):503–514. doi: [10.1089/ten.tea.2016.0418](https://doi.org/10.1089/ten.tea.2016.0418)
61. Oberdiek F, Vargas CI, Rider P, et al. Ex vivo and in vivo analyses of novel 3d-printed bone substitute scaffolds incorporating biphasic calcium phosphate granules for bone regeneration. *Int J Mol Sci.* 2021;22(7):3588. doi: [10.3390/ijms22073588](https://doi.org/10.3390/ijms22073588)
62. Seidenstuecker M, Lange S, Esslinger S, et al. Inversely 3D-printed β-TCP scaffolds for bone replacement. *Materials.* 2019;12(20):3417. doi: [10.3390/ma12203417](https://doi.org/10.3390/ma12203417)
63. Bruyas A, Lou F, Stahl AM, et al. Systematic characterization of 3D-printed PCL/β-TCP scaffolds for biomedical devices and bone tissue engineering: influence of composition and porosity. *J Mater Res.* 2018;33(14):1948–1959. doi: [10.1557/jmr.2018.112](https://doi.org/10.1557/jmr.2018.112)
64. Liu D, Nie W, Li D, et al. 3D printed PCL/SrHA scaffold for enhanced bone regeneration. *Chem Eng J.* 2019;362:269–279. doi: [10.1016/j.cej.2019.01.015](https://doi.org/10.1016/j.cej.2019.01.015)
65. Grigora M-E, Terzopoulou Z, Baciu D, et al. 3D printed poly(lactic acid)-based nanocomposite scaffolds with bioactive coatings for tissue engineering applications. *J Mater Sci.* 2023;58(6):2740–2763. doi: [10.1007/s10853-023-08149-4](https://doi.org/10.1007/s10853-023-08149-4)
66. Nazeer MA, Onder OC, Sevgili I, et al. 3D printed poly(lactic acid) scaffolds modified with chitosan and hydroxyapatite for bone repair applications. *Mater Today Commun.* 2020;25:101515. doi: [10.1016/j.mtcomm.2020.101515](https://doi.org/10.1016/j.mtcomm.2020.101515)
67. Wang W, Liu P, Zhang B, et al. Fused deposition modeling printed PLA/Nano β-TCP composite bone tissue engineering scaffolds for promoting osteogenic induction function. *Int J Nanomedicine.* 2023;18(October):5815–5830. doi: [10.2147/IJN.S416098](https://doi.org/10.2147/IJN.S416098)
68. Dey M, Ozbolat IT. 3D bioprinting of cells, tissues and organs. *Sci Rep.* 2020;10(1):10–12. doi: [10.1038/s41598-020-70086-y](https://doi.org/10.1038/s41598-020-70086-y)

69. Gungor-Ozkerim PS, Inci I, Zhang YS, et al. Bioinks for 3D bioprinting: an overview. *Biomater Sci*. 2018;6(5):915–946. doi: [10.1039/C7BM00765E](https://doi.org/10.1039/C7BM00765E)
70. Filardo G, Petretta M, Cavallo C, et al. Patient-specific meniscus prototype based on 3D bioprinting of human cell-laden scaffold. *Bone Joint Res*. 2019;8(2):101–106. doi: [10.1302/2046-3758.82.BJR-2018-0134.R1](https://doi.org/10.1302/2046-3758.82.BJR-2018-0134.R1)
71. Gao G, Schilling AF, Hubbell K, et al. Improved properties of bone and cartilage tissue from 3D inkjet-bioprinted human mesenchymal stem cells by simultaneous deposition and photocrosslinking in PEG-GelMA. *Biotechnol Lett*. 2015;37(11):2349–2355. doi: [10.1007/s10529-015-1921-2](https://doi.org/10.1007/s10529-015-1921-2)
72. Zheng XQ, Huang JF, Lin JL, et al. 3D bioprinting in orthopedics translational research. *J Biomater Sci Polym Ed*. 2019;30(13):1172–1187. doi: [10.1080/09205063.2019.1623989](https://doi.org/10.1080/09205063.2019.1623989)
73. Kang Y, Xu J, Meng L, et al. 3D bioprinting of dECM/Gel/QCS/nHAp hybrid scaffolds laden with mesenchymal stem cell-derived exosomes to improve angiogenesis and osteogenesis. *Biofabrication*. 2023;15(2):024103. doi: [10.1088/1758-5090/acb6b8](https://doi.org/10.1088/1758-5090/acb6b8)
74. Shen M, Wang L, Gao Y, et al. 3D bioprinting of in situ vascularized tissue engineered bone for repairing large segmental bone defects. *Mater Today Bio*. 2022;16(June):100382. doi: [10.1016/j.mtbio.2022.100382](https://doi.org/10.1016/j.mtbio.2022.100382)
75. Guo C, Wu J, Zeng Y, et al. Construction of 3D bioprinting of HAP/collagen scaffold in gelatin bath for bone tissue engineering. *Regen Biomater*. 2023;10(August). doi: [10.1093/rb/rbad067](https://doi.org/10.1093/rb/rbad067)
76. Touya N, Devun M, Handschin C, et al. In vitro and in vivo characterization of a novel tricalcium silicate-based ink for bone regeneration using laser-assisted bioprinting. *Biofabrication*. 2022;14(2):024104. doi: [10.1088/1758-5090/ac584b](https://doi.org/10.1088/1758-5090/ac584b)
77. K erour dan O, Hakobyan D, R emy M, et al. In situ prevascularization designed by laser-assisted bioprinting: effect on bone regeneration. *Biofabrication*. 2019;11(4):045002. doi: [10.1088/1758-5090/ab2620](https://doi.org/10.1088/1758-5090/ab2620)
78. Keriquel V, Oliveira H, R emy M, et al. In situ printing of mesenchymal stromal cells, by laser-assisted bioprinting, for in vivo bone regeneration applications. *Sci Rep*. 2017;7(1):1778. doi: [10.1038/s41598-017-01914-x](https://doi.org/10.1038/s41598-017-01914-x)
79. Khalaf AT, Wei Y, Wan J, et al. Bone tissue engineering through 3D bioprinting of bioceramic scaffolds: a review and update. *Life*. 2022;12(6):903–928. doi: [10.3390/life12060903](https://doi.org/10.3390/life12060903)
80. Zhang B, Wang L, Song P, et al. 3D printed bone tissue regenerative PLA/HA scaffolds with comprehensive performance optimizations. *Mater Des*. 2021;201:109490. doi: [10.1016/j.matdes.2021.109490](https://doi.org/10.1016/j.matdes.2021.109490)
81. Wang W, Zhang B, Li M, et al. 3D printing of PLA/n-HA composite scaffolds with customized mechanical properties and biological functions for bone tissue engineering. *Compos B Eng*. 2021;224:109192. doi: [10.1016/j.compositesb.2021.109192](https://doi.org/10.1016/j.compositesb.2021.109192)
82. Bilgili HK, Aydin MS, Sahin M, et al. 3D-Printed functionally graded PCL-HA scaffolds with multi-scale porosity. *ACS Omega*. 2025;10(7):6502–6519. doi: [10.1021/acsomega.4c06820](https://doi.org/10.1021/acsomega.4c06820)
83. Wang F, Tankus EB, Santarella F, et al. Fabrication and characterization of PCL/HA filament as a 3D printing material using thermal extrusion technology for bone tissue engineering. *Polym (Basel)*. 2022;14(4):669. doi: [10.3390/polym14040669](https://doi.org/10.3390/polym14040669)
84. Jiao Z, Luo B, Xiang S, et al. 3D printing of HA/PCL composite tissue engineering scaffolds. *Adv Ind Eng Polym Res*. 2019;2(4):196–202. doi: [10.1016/j.aiepr.2019.09.003](https://doi.org/10.1016/j.aiepr.2019.09.003)
85. Cestari F, Petretta M, Yang Y, et al. 3D printing of PCL/nano-hydroxyapatite scaffolds derived from biogenic sources for bone tissue engineering. *Sustain Mater Technol*. 2021;29:e00318. doi: [10.1016/j.susmat.2021.e00318](https://doi.org/10.1016/j.susmat.2021.e00318)
86. Aihemaiti P, Jiang H, Aiyiti W, et al. Mechanical properties enhancement of 3D-printed HA-PLA composites using ultrasonic vibration assistance. *Virtual Phys Prototyp*. 2024;19(1). doi: [10.1080/17452759.2024.2346271](https://doi.org/10.1080/17452759.2024.2346271)
87. Raziyan MS, Palevicius A, Perkowski D, et al. Development and evaluation of 3D-Printed PLA/PHA/PHB/HA composite scaffolds for enhanced tissue-engineering applications. *J Compos Sci*. 2024;8(6):226. doi: [10.3390/jcs8060226](https://doi.org/10.3390/jcs8060226)
88. Rstakyan V, Mkhitarian L, Baghdasaryan L, et al. Stereolithography of ceramic scaffolds for bone tissue regeneration: influence of hydroxyapatite/silica ratio on mechanical properties. *J Mech Behav Biomed Mater*. 2024;152:106421. doi: [10.1016/j.jmbbm.2024.106421](https://doi.org/10.1016/j.jmbbm.2024.106421)
89. Kim J-W, Yang B-E, Hong S-J, et al. Bone regeneration capability of 3D printed ceramic scaffolds. *Int J Mol Sci*. 2020;21(14):4837. doi: [10.3390/ijms21144837](https://doi.org/10.3390/ijms21144837)
90. Baino F, Magnaterra G, Fiume E, et al. Digital light processing stereolithography of hydroxyapatite scaffolds with bone-like architecture, permeability, and mechanical properties. *J Am Ceram Soc*. 2022;105(3):1648–1657. doi: [10.1111/jace.17843](https://doi.org/10.1111/jace.17843)
91. Elhattab K, Bhaduri SB, Sikder P. Influence of fused deposition modelling nozzle temperature on the rheology and mechanical properties of 3D printed β -tricalcium phosphate (TcP)/polylactic acid (PLA) composite. *Polym (Basel)*. 2022;14(6):1222. doi: [10.3390/polym14061222](https://doi.org/10.3390/polym14061222)
92. Won J-Y, Park C-Y, Bae J-H, et al. Evaluation of 3D printed PCL/PLGA/ β -TCP versus collagen membranes for guided bone regeneration in a beagle implant model. *Biomed Mater*. 2016;11(5):055013. doi: [10.1088/1748-6041/11/5/055013](https://doi.org/10.1088/1748-6041/11/5/055013)
93. Zheng C, Zhang M. 3D-printed PCL/ β -TCP/CS composite artificial bone and histocompatibility study. *J Orthop Surg Res*. 2023;18(1):981. doi: [10.1186/s13018-023-04489-8](https://doi.org/10.1186/s13018-023-04489-8)
94. Lindner M, Hoeges S, Meiners W, et al. Manufacturing of individual biodegradable bone substitute implants using selective laser melting technique. *J Biomed Mater Res A*. 2011;97A(4):466–471. doi: [10.1002/jbm.a.33058](https://doi.org/10.1002/jbm.a.33058)
95. Song S, Gao Z, Xu H, et al. Rapid preparation and performance of degradable ceramic scaffolds based on stereolithography. *J Asian Ceramic Soc*. 2022;10(1):58–68. doi: [10.1080/21870764.2021.2008102](https://doi.org/10.1080/21870764.2021.2008102)
96. Wang B, Ye X, Chen G, et al. Fabrication and properties of PLA/ β -TCP scaffolds using liquid crystal display (LCD) photocuring 3D printing for bone tissue engineering. *Front Bioeng Biotechnol*. 2024;12:12. doi: [10.3389/fbioe.2024.1273541](https://doi.org/10.3389/fbioe.2024.1273541)
97. Tarafder S, Bose S. Polycaprolactone-coated 3D printed tricalcium phosphate scaffolds for bone tissue engineering: *in vitro* alendronate release behavior and local delivery effect on *in vivo* osteogenesis. *ACS Appl Mater Interfaces*. 2014;6(13):9955–9965. doi: [10.1021/am501048n](https://doi.org/10.1021/am501048n)
98. Zhang B, Sun H, Wu L, et al. 3D printing of calcium phosphate bioceramic with tailored biodegradation rate for skull bone tissue reconstruction. *Bio-des Manuf*. 2019;2(3):161–171. doi: [10.1007/s42242-019-00046-7](https://doi.org/10.1007/s42242-019-00046-7)
99. Kim Y, Lim JY, Yang GH, et al. 3D-printed PCL/bioglass (BGS-7) composite scaffolds with high toughness and cell-responses for bone tissue regeneration. *J Ind Eng Chem*. 2019;79:163–171. doi: [10.1016/j.jiec.2019.06.027](https://doi.org/10.1016/j.jiec.2019.06.027)
100. Wang C, Meng C, Zhang Z, et al. 3D printing of polycaprolactone/bioactive glass composite scaffolds for in situ bone repair. *Ceram Int*. 2022;48(6):7491–7499. doi: [10.1016/j.ceramint.2021.11.293](https://doi.org/10.1016/j.ceramint.2021.11.293)
101. Zhang C, Chen S, Vigneshwaran M, et al. Effect of different contents of 63s Bioglass on the performance of Bioglass-PCL composite bone scaffolds. *Inventions*. 2023;8(6):138. doi: [10.3390/inventions8060138](https://doi.org/10.3390/inventions8060138)
102. Daskalakis E, Huang B, Vyas C, et al. Novel 3D bioglass scaffolds for bone tissue regeneration. *Polym (Basel)*. 2022;14(3):445. doi: [10.3390/polym14030445](https://doi.org/10.3390/polym14030445)
103. Sch atzlein E, Kicker C, S ohling N, et al. 3D-Printed PLA-Bioglass scaffolds with controllable calcium release and MSC adhesion for bone tissue engineering. *Polym (Basel)*. 2022;14(12):2389. doi: [10.3390/polym14122389](https://doi.org/10.3390/polym14122389)
104. Kolan KCR, Leu MC, Hilmas GE, et al. Fabrication of 13–93 bioactive glass scaffolds for bone tissue engineering using indirect selective laser sintering. *Biofabrication*. 2011;3(2):025004. doi: [10.1088/1758-5082/3/2/025004](https://doi.org/10.1088/1758-5082/3/2/025004)

105. Budharaju H, Suresh S, Sekar MP, et al. Ceramic materials for 3D printing of biomimetic bone scaffolds – current state-of-the-art & future perspectives. *Mater Des.* 2023;231:112064. doi: [10.1016/j.matdes.2023.112064](https://doi.org/10.1016/j.matdes.2023.112064)
106. Yamada M, Shiota M, Yamashita Y, et al. Histological and histomorphometrical comparative study of the degradation and osteoconductive characteristics of α - and β -tricalcium phosphate in block grafts. *J Biomed Mater Res B Appl Biomater.* 2007;82B(1):139–148. doi: [10.1002/jbm.b.30715](https://doi.org/10.1002/jbm.b.30715)
107. Tronco MC, Cassel JB, dos Santos LA. α -TCP-based calcium phosphate cements: a critical review. *Acta Biomater.* 2022;151:70–87. doi: [10.1016/j.actbio.2022.08.040](https://doi.org/10.1016/j.actbio.2022.08.040)
108. Saijo H, Igawa K, Kanno Y, et al. Maxillofacial reconstruction using custom-made artificial bones fabricated by inkjet printing technology. *J Artif Organs.* 2009;12(3):200–205. doi: [10.1007/s10047-009-0462-7](https://doi.org/10.1007/s10047-009-0462-7)
109. Saijo H, Fujihara Y, Kanno Y, et al. Clinical experience of full custom-made artificial bones for the maxillofacial region. *Regen Ther.* 2016;5:72–78. doi: [10.1016/j.reth.2016.08.004](https://doi.org/10.1016/j.reth.2016.08.004)
110. Kobbe P, Laubach M, Hutmacher DW, et al. Convergence of scaffold-guided bone regeneration and RIA bone grafting for the treatment of a critical-sized bone defect of the femoral shaft. *Eur J Med Res.* 2020;25(1):1–12. doi: [10.1186/s40001-020-00471-w](https://doi.org/10.1186/s40001-020-00471-w)
111. Castrisos G, Gonzalez Matheus I, Sparks D, et al. Regenerative matching axial vascularisation of absorbable 3D-printed scaffold for large bone defects: a first in human series. *J Plast Reconstructive Aesthetic Surg.* 2022;75(7):2108–2118. doi: [10.1016/j.bjps.2022.02.057](https://doi.org/10.1016/j.bjps.2022.02.057)
112. Jeong WS, Kim YC, Min JC, et al. Clinical application of 3D-Printed patient-specific Polycaprolactone/Beta tricalcium phosphate scaffold for complex zygomatico-maxillary defects. *Polym (Basel).* 2022;14(4):740. doi: [10.3390/polym14040740](https://doi.org/10.3390/polym14040740)
113. Park H, Choi JW, Jeong WS. Clinical application of three-dimensional printing of Polycaprolactone/Beta-tricalcium phosphate implants for cranial reconstruction. *J Craniofacial Surg.* 2022;33(5):1394–1399. doi: [10.1097/SCS.00000000000008595](https://doi.org/10.1097/SCS.00000000000008595)
114. Khotib J, Lasandara CS, Samirah, et al. Acceleration of bone fracture healing through the use of natural bovine hydroxyapatite implant on bone defect animal model. *Folica Medica Indonesiana.* 2019;55(3):176–187. doi: [10.20473/fmi.v55i3.15495](https://doi.org/10.20473/fmi.v55i3.15495)
115. Gani MA, Lee G, Ardianto C, et al. Comparative study of bovine and synthetic hydroxyapatite in micro- and nanosized on osteoblasts action and bone growth. *Papaccio G, editor. PLoS One.* 2025;20(1):e0311652. doi: [10.1371/journal.pone.0311652](https://doi.org/10.1371/journal.pone.0311652)
116. Bansal S, Chauhan V, Sharma S, et al. Evaluation of hydroxyapatite and beta-tricalcium phosphate mixed with bone marrow aspirate as a bone graft substitute for posterolateral spinal fusion. *Indian J Orthop.* 2009;43(3):234–239. doi: [10.4103/0019-5413.49387](https://doi.org/10.4103/0019-5413.49387)
117. Ye X, Cai S, Xu G, et al. Preparation and in vitro evaluation of mesoporous hydroxyapatite coated β -TCP porous scaffolds. *Mater Sci Eng: C.* 2013;33(8):5001–5007. doi: [10.1016/j.msec.2013.08.027](https://doi.org/10.1016/j.msec.2013.08.027)
118. Ramakrishnan P, Nagarajan S, Thiruvengadam V, et al. Cation doped hydroxyapatite nanoparticles enhance strontium adsorption from aqueous system: a comparative study with and without calcination. *Appl Clay Sci.* 2016;134:136–144. doi: [10.1016/j.clay.2016.09.022](https://doi.org/10.1016/j.clay.2016.09.022)
119. Li C, Sun F, Tian J, et al. Continuously released Zn²⁺ in 3D-printed PLGA/ β -TCP/Zn scaffolds for bone defect repair by improving osteoinductive and anti-inflammatory properties. *Bioact Mater.* 2023;24:361–375. doi: [10.1016/j.bioactmat.2022.12.015](https://doi.org/10.1016/j.bioactmat.2022.12.015)
120. Mehrjoo M, Javadpour J, Ali Shokrgozar M, et al. Effect of magnesium substitution on structural and biological properties of synthetic hydroxyapatite powder. *Mat Express.* 2015;5(1):41–48. doi: [10.1166/mex.2015.1205](https://doi.org/10.1166/mex.2015.1205)
121. Santos GG, Nunes VLC, Marinho SMOC, et al. Biological behavior of magnesium-substituted hydroxyapatite during bone repair. *Braz J Biol.* 2021;81(1):53–61. doi: [10.1590/1519-6984.217769](https://doi.org/10.1590/1519-6984.217769)
122. Li C, Sun F, Tian J, et al. Continuously released Zn²⁺ in 3D-printed PLGA/ β -TCP/Zn scaffolds for bone defect repair by improving osteoinductive and anti-inflammatory properties. *Bioact Mater [Internet].* 2023;24:361–375. doi: [10.1016/j.bioactmat.2022.12.015](https://doi.org/10.1016/j.bioactmat.2022.12.015)
123. Wang W, Wei J, Lei D, et al. 3D printing of lithium osteogenic bioactive composite scaffold for enhanced bone regeneration. *Compos B Eng.* 2023;256:110641. doi: [10.1016/j.compositesb.2023.110641](https://doi.org/10.1016/j.compositesb.2023.110641)
124. Carter DR, Hayes WC. Bone compressive strength: the influence of density and strain rate. *Sci (1979).* 1976;194(4270):1174–1176. doi: [10.1126/science.996549](https://doi.org/10.1126/science.996549)
125. Lu L, Zhang Q, Wootton DM, et al. Mechanical study of polycaprolactone-hydroxyapatite porous scaffolds created by Porogen-based solid freeform fabrication method. *J Appl Biomater Funct Mater.* 2014;12(3):145–154. doi: [10.5301/jabfm.5000163](https://doi.org/10.5301/jabfm.5000163)
126. Probst FA, Hutmacher DW, Müller DF, et al. Rekonstruktion der Kalvaria durch ein präfabriziertes bioaktives Implantat. *Handchir Mikrochir Plast Chir.* 2010;42(6):369–373. doi: [10.1055/s-0030-1248310](https://doi.org/10.1055/s-0030-1248310)
127. Athanasiou K. Sterilization, toxicity, biocompatibility and clinical applications of polylactic acid/polyglycolic acid copolymers. *Biomaterials.* 1996;17(2):93–102. doi: [10.1016/0142-9612\(96\)85754-1](https://doi.org/10.1016/0142-9612(96)85754-1)
128. International Organization for Standardization. Biological evaluation of medical devices. Biological evaluation of medical devices 10993. Geneva (Switzerland): ISO; 2020.
129. Ninarello D, Ballardini A, Morozzi G, et al. A comprehensive systematic review of marketed bone grafts for load-bearing critical-sized bone defects. *J Mech Behav Biomed Mater.* 2024;160:106782. doi: [10.1016/j.jmbbm.2024.106782](https://doi.org/10.1016/j.jmbbm.2024.106782)
130. Slavin BV, Ehlen QT, Costello JP, et al. 3D printing applications for craniomaxillofacial reconstruction: a sweeping review. *ACS Biomater Sci Eng.* 2023;9(12):6586–6609. doi: [10.1021/acsbomaterials.3c01171](https://doi.org/10.1021/acsbomaterials.3c01171)
131. Morrison RJ, Kashlan KN, Flanagan CL, et al. Regulatory considerations in the design and manufacturing of implantable 3D-Printed medical devices. *Clin Transl Sci.* 2015;8(5):594–600. doi: [10.1111/cts.12315](https://doi.org/10.1111/cts.12315)